INTERNAL DEBONDING OF SOLID ROCKET FUEL: AN EXPERIMENTAL INVESTIGATION

THESIS

James N. Hanley
Captain, USAF

AFIT/GAE/AA/88D-19

DEPARTMENT OF THE AIR FORCE
AIR UNIVERSITY
AIR FORCE INSTITUTE OF TECHNOLOGY
Wright-Patterson Air Force Base, Ohio

AFIT/GAE/AA/88D-19

INTERNAL DEBONDING OF SOLID ROCKET FUEL:

AN EXPERIMENTAL INVESTIGATION

THESIS

James N. Hanley
Captain, USAF

AFIT/GAE/AA/88D-19

Approved for public release; distribution unlimited

AFIT/GAE/AA/88D-19

INTERNAL DEBONDING OF SOLID ROCKET FUEL: AN EXPERIMENTAL INVESTIGATION

THESIS

Presented to the Faculty of the School of Engineering

of the Air Force Institute of Technology

Air University

In Partial Fulfillment of the

Requirements for the Degree of

Master of Science in Aeronautical Engineering

James N. Hanley, B.S.

Captain, USAF

December 1988

Preface

The major purpose of this thesis was to develop a blister test to measure the debond fracture energy in a solid rocket fuel. I could not have accomplished this without the help of Jay Anderson. Jay helped with the assembly and connection of the test equipment and trouble shooting of the equipment.

I wish to thank my faculty advisor, Maj. Paul Copp, for his time and assistance in completing this project. I have learned a great deal from him. I wish to also thank the Air Force Astronautics Laboratory, AFAL/MKPB, Edwards Air Force Base for the lab's assistance in obtaining the adhesive chemicals and providing the testing to determine the adhesive's material properties. In particular I wish to thank Dr. Heidi Schreuder-Stacer for her advice and help in analyzing the experimental results. This is dedicated to my parents who live in the world champion city, home of the Lakers and the Dodgers.

Table of Contents

List of Figures

List of Tables

List of Symbols

a	radius of blister
D	plate flexural rigidity
E	Young's modulus
G_a	adhesive fracture energy
h	blister height deflection
M	moment
p	pressure
r	radial location from center of blister
S	surface area
t	thickness of adhesive
$w(r)$	deflection as a function of radial direction
x	axial location
$\delta()$	virtual (work or displacement)
ν	Poisson's ratio

Abstract

The objective of this study was the development of a method to compute the fracture energy required to debond crystal particles in a solid rocket fuel. A blister test was defined that pressurizes an initially debonded region to generate an adhesive fracture. An LVDT measures the displacement of the blister. The fracture energy is expressed in terms of the critical loading, displacement, specimen geometry and material properties. Consistent results required developing a proper casting and curing method for thin polymeric layers onto a crystal substrate. Various thicknesses and substrates were examined.

The study found that the deflection of the blister behaved like a plate and could be analyzed as one to compute the adhesive fracture energy. The dimensionless values of fracture energy fell along predictable curves for small values of adhesive thicknesses to blister radii. The adhesive fracture energy was found to be a function of the force applied, adhesive material properties and the blister geometry.

The value for adhesive fracture energy on a crystal substrate is compared to a Plexiglass substrate for an epoxy resin. Both a polished and unpolished crystal specimen's fracture energy are compared.

INTERNAL DEBONDING OF SOLID ROCKET FUEL: AN EXPERIMENTAL INVESTIGATION

I. Introduction

Objective

The main objective of this research was to develop a blister test technique to measure the debond fracture energy of an elastomeric material from a crystalline material. The test developed should have the following properties. It should use a simple specimen and the failure load should remain constant so that the average strength of the adhesive can be determined. The adhesive fracture energy, G_a, should be expressed directly in terms of the specimen dimensions, its stiffness, and the critical load.

The test will involve developing the appropriate casting technique to ensure a consistently cured layer of elastomeric material with uniform thickness over the crystalline substrate. A precracking or initial debonding method must be devised, as well as, a method to measure the critical pressure and blister height. Finally, the test should determine the interfacial adhesive debonding energy between

the elastomeric material and the crystalline substrate. It is important that the elastomer and crystal substrate be typical components of solid rocket fuels.

Background

Ammonia per chlorate (AP) is used in solid rocket fuel to control the burn rate of the aluminum crystals and their matrix. Fine particles of AP will increase the burn rate and larger ones will decrease the burn rate. It is required to find the energy holding these AP crystals in the fuel matrix to keep the burn rate constant for a particular stage of the fuel. This is to prevent fracturing the crystal and creating uneven burning which could lead to an explosive failure of the rocket casing [15].

Fracture in a solid rocket engine composed of an elastomeric fuel filled with a hard crystalline particulate oxidizer may occur in two major modes. First it can progress along the original interface, between the substrate and the polymer matrix layer, called adhesive fracture. Alternatively, it can progress through the polymeric boundary layer by the separation of the material from itself, called cohesive fracture, [5: 125]. The mode that occurs depends upon the strain rate applied and the geometry of the adhesive. There has been some discussion on whether fracture energy is a material constant or not. According to Bennett,

De Vries and Williams [3: 34] cohesive fracture energy is a material property independent of specimen geometry, however adhesive fracture energy depends on surface preparation and is not a material property. While others have found adhesive energy to be a material property. Malyshev and Salganik used a point-loaded circular plate for their blister test and found that adhesive fracture energy is a material constant with a limitation. The best correlation of G_a as a material constant occurred when the deflections were smaller than the adhesive thickness. In such cases, the experiment remains within the limitations of the basic plate theory [3: 33,36]. An understanding of the adhesive fracture involves an evaluation of the energy required to separate the crystal from the matrix.

A variety of tests have been proposed to measure the adhesive fracture energy. Tests to determine the fracture energy include the peel test, shear tests, cleavage tests, tension tests, and blister tests. These tests all have their advantages and disadvantages.

The peel test is the most widely used technique. In the peel test the adhesive is applied between a rigid substrate and a flexible member at an angle of either 90° or 180° from the rigid member. Failure in the peel test may occur in the flexible member, in the adhesive or in the rigid member. Because of this, adhesive fracture might not be measured in the experiment. The stress distribution in the peel test is

complex. The force required to initiate and maintain the peeling of the flexible member from the rigid one is influenced by the width of the specimen, the mechanical properties of the substrate and the strength of the adhesive. Because a very small change in the adhesive thickness will give a large variation in peel force, only an average force over the entire length of the specimen is computed from each test [17: 99]. The major deficiency lies in the data acquisition and reduction. Load and displacement data are taken relative to the cross head motions of the load and not in the area where fracture is occurring. Thus a number of phenomena are occurring together that complicate calculation of the fracture energy from the data. The mechanics models used for these tests can only provide average values.

A variety of shear tests have been used to find fracture energy. The test requires the adhesive to be applied to two substrates. Then the overlapping substrates are pulled in opposite directions causing the substrates to slide apart. The shear test computes the total of the specific fracture energy and mechanical adhesion [13: 214]. Mechanical adhesion is the bonding force provided by interlocking action of the two surfaces and is most effective under shear loading and contributes little to tensile strength [13: 211]. The major disadvantage in this test is that the test computes the total fracture energy, including the mechanical adhesion energy. It would also be difficult to mount the crystal

substrates in the test equipment and keep them properly aligned without breaking the crystals.

There are numerous cleavage tests that have been used to compute adhesive fracture energy in epoxy resins. Values of G_a ranged from 0.571 to 57.1 Lbf * in/ in^2 [16: 22] [12: 2000] [2: 338, 334] [4: 591]. The cleavage test introduces a prying force at one end of a bonded specimen to split the bond apart. Again the adhesive is applied between two crystal substrates and the difficulty in pulling them apart has been mentioned above. The cleavage test includes mechanical adhesion in its measurement of G_a so its values will be high [13: 210-211]. The cantilever split beam test first used by Berry is used to evaluate fracture energy in thin sheets. An advantage of this test is that it uses simple beam theory. This test however, is best suited for cohesive fracture and not for adhesive fracture [21: 32].

In the tensile test two substrates are joined by the adhesive and are pulled apart perpendicular to the adhesive plane. This test gives the maximum tensile load per unit area to cause debond. In this test mechanical adhesion contributes very little to the total fracture energy. But again, there is the need to apply force to two crystals that are easy to break.

Dr. M. L. Williams proposed a pressurized blister test that allows a more precise measurement of data at the fracture site based on the Griffith energy balance analysis

[7:5]. Griffith first used an energy balance between the strain energy released and the increase in surface energy with crack growth. His prediction of a finite critical stress to initiate fracture of a central finite length crack was in an infinite elastic sheet under tension. Griffith's stress equals $(2 E G_c / \pi a)^{1/2}$, where G_c is cohesive fracture energy [3:34].

The blister test consists of a plate bonded to a rigid substrate, except for a central portion of radius a_o. When the unbonded region is pressurized the plate lifts off the substrate and forms a 'blister'. Figure 1 shows an example of the formed blister. The radius of the blister remains fixed as its height grows until a critical pressure, p_{cr}, is reached. At this pressure the radius of the blister increases in size. The debonding mechanism is an adhesive failure along the interface, and crack growth occurs. Advantages of the blister test are: (1) the specimens are reasonably simple to prepare, (2) the tests are easily conducted with inexpensive equipment, (3) a large range of specimen thicknesses or diameters can be examined and (4) a variety of debond radii can be used. In addition, it is often possible to obtain several data points from a single test specimen [2:41].

The blister test has an advantage over the cantilever beam test. There is no need to control debonding along a straight initial fracture surface in the blister test. This

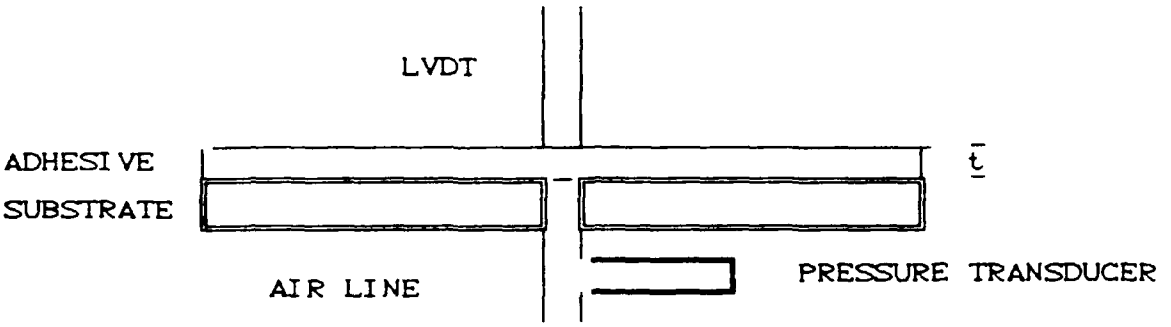

a. Initial Blister set-up

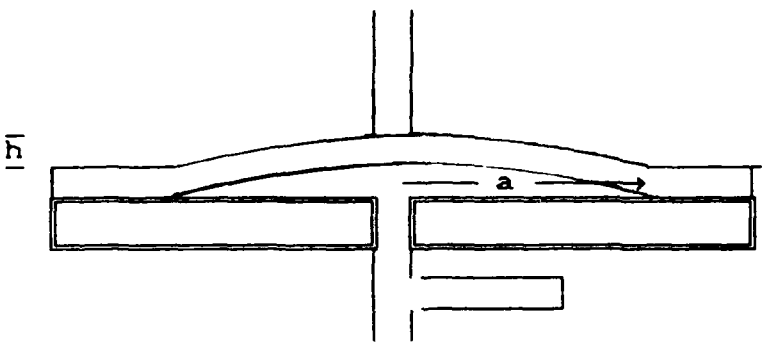

b. Formed Blister

Figure 1. Blister Set up and Formed Blister

is because there are no "sides" on a circular specimen as there are when bonding two beam substrates together and the fracture should occur along the natural interface of crystal and elastomer material [21: 36]. The same may be said for the cleavage, shear and tension tests. Mathematically infinite stresses exist at the bonded end of the cantilever beam or at the clamped edge of the specimen-bond interface. These infinite stresses are not used in computing G_a and this contributes to the potential error in determining the adhesive fracture energy.

The blister test does not use a concentrated load but a distributed load over the region of debond. This should avoid cohesive fracture and puncture of the adhesive because the load is applied symmetrically and uniformly. Also there is less need to have the debond area remain concentric over the center of the specimen because the deflection measuring device may be readjusted to the center of the blister. The blister test will be used in this experiment because of its advantages and the disadvantages of the other tests.

The blister test has been used to compute adhesive fracture energy in epoxy resins and adhesive tapes. Andrews and Stevenson found values of 0.228 to 2.284 $Lbf*in/in^2$ and for the same epoxy King and Andrews found a value of 0.0171 $Lbf * in/ in^2$ [1: 1681, 1686, 1687]. The pressure rates used by Andrews and Stevenson were between 10 to 10^6 psi/sec. They found that for an increase in pressurization rate the

adhesive fracture energy also increased. Gent computed adhesive fracture energy for 3-M Tape on plexiglass with values of 0.120 to 0.148 Lbf*in/in^2 and on a teflon substrate from 0.857 to 0.879 Lbf*in/in^2 [6: 18]. It should be noted from these results that the fracture energy for a given material can vary by two orders of magnitude, a factor of one hundred. However it is usually in the range of 0.12 to 2.30 Lbf * in/ in^2.

Theory

The adhesive fracture energy in the blister test is computed from the principle of energy conservation. The work done by the applied pressure moving through the virtual displacement must be balanced by the change in internal strain energy plus the change in energy needed to create any new surface [21: 30]. In equilibrium the virtual work should equal the virtual internal energy shown below

$$\delta(U-A) = \delta(\pi * a^2 * G_a) \qquad (1)$$

where U is strain energy, A is surface energy, and a is the radius of the crack or blister . The change in internal elastic strain energy stored is one half the applied work for a linear load deflection relation by Clapeyron's Theorem [10: 27]. The work applied for a linear system is:

$$\text{Work} = 2\pi \int_0^a p\, w(r)\, r\, dr \qquad (2)$$

p = pressure

$w(r)$ = deflection in the plane perpendicular to the area of interest

r = radius

Applying Clapeyron's Theorem to Equation 2 and setting the work equal to the internal energy in Equation 1 the result is

$$\delta \left(\frac{1}{2} * 2\pi \int_0^a p\, w(r)\, r\, dr \right) = \delta \left(\pi a^2 G_a \right) \qquad (3)$$

To find the deflection, $w(r)$, of a plate it is necessary to look at the bending moment at any cross section. The equation for the bending moment is

$$M = \frac{Plx}{2} - \frac{P x^2}{2} - Sw + M_o \qquad (4)$$

M = bending moment

x = distance along x axis

S = surface area

M_o = internal moment

The bending moment is also equal to

$$M = - D \frac{d^2w}{dx^2} \qquad (5)$$

D = flexural rigidity

$\frac{d^2w}{dx^2}$ = curvature of the plate

Combining Equations 4 and 5 and rewriting them yields

$$\frac{d^2w}{dx^2} - \frac{Sw}{D} = \frac{Plx}{2D} + \frac{Px^2}{2D} - \frac{M_o}{D} \qquad (6)$$

The general solution for the displacement, w, in the z axis direction can be found to be [10: 7]

$$w = C_1 \sinh\left(\frac{2\mu x}{l}\right) + C_2 \cosh\left(\frac{2\mu x}{l}\right) + \frac{Pl\,x^3}{8\mu^2 D} - \frac{Pl^2x^2}{8\mu^2 D} - \frac{Pl^4}{16\mu^4 D} + \frac{M_o l^2}{4\mu^2 D} \qquad (7)$$

using $\mu^2 = \frac{Sl^2}{4D}$

Symmetry is used to solve for the constants. For the plate the displacement equals zero at the clamped end and the slope at the center and clamped end also equals zero. Using these three boundary conditions we can solve for C_1, C_2, and M_o.

$$C_1 = \frac{-pl^4}{16\mu^3 D} \quad ; \quad C_2 = \frac{pl^4}{16\mu^3 D} \coth \mu \quad ; \quad M_o = \frac{-pl^2}{12} \Psi_1(\mu) \qquad (8)$$

The maximum deflection will be in the middle of the

plate and using symmetry this deflection will be:

$$w_{max} = \frac{pl^4}{384D} f_1(\mu) \tag{9}$$

For a uniformly loaded circular plate the deflection was found by Timoshenko to be [10: 54]

$$w = \frac{pr^4}{64D} + \frac{C_1 r^2}{4} + C_2 \ln \frac{r}{a} + C_3 \tag{10}$$

for a plate with clamped edges and the boundary conditions listed above. Using the boundary conditions to solve this equation the displacement is

$$w = \frac{p}{64D}(a^2 - r^2)^2 \tag{11}$$

The deflection will be a maximum at the center where r equals zero. Thus, the maximum deflection is

$$w_{max} = \frac{pa^4}{64D} \tag{12}$$

The equation for virtual work may now be expressed as

$$\delta(\pi a^2 G_a) = \delta\left(\pi \int_0^a p \left(\frac{p}{64D}(a^2 - r^2)^2\right) r\, dr\right) \tag{13}$$

Solving this equation for pressure, p, the solution as found by Timoshenko is

$$p = \left[\frac{128GD}{a^4}\right]^{\frac{1}{2}} = \left[\frac{32\ h^3 E\ G}{3(1-\nu^2)a^4}\right]^{\frac{1}{2}} \qquad (14)$$

The strain energy required to debond a plate from a substrate is then

$$G_a = \frac{(1-\nu^2)a^4 p^2}{32\ h^3\ E} \qquad (15)$$

This equation for fracture energy should be good in the blister test when there are only small deflections in the adhesive plate. A more complete solution for the adhesive fracture energy may be found by using applied stresses. The energy release rate can come from a combination of both near and far field stresses. The near field stress is the stress field around the internal crack and the far field stress is due to the global deflection of the plate [1:1683]. For an infinitely thick plate the far field energy will approach zero because the plate is too thick to bend or deform.

For a penny-shaped crack subject to internal pressure Sneddon [18: 138] found the near field energy to be

$$G_n = \frac{8(1-\nu^2)}{3E} p^2 a^3 \qquad (16)$$

If the crack is at the interface of a rigid substrate then the near field energy will be half the value in Equation 16, and therefore for the blister test one obtains

$$G_n = \frac{4(1-n^2)}{3E} p^2 a^3 \qquad (17)$$

Timoshenko and Goodier [19: 40] found the far field stresses in a thick shell to be

$$\sigma_r = \frac{-6p}{h^3}\left(r^2 z - \frac{2z^3}{3}\right)$$

$$\sigma_z = \frac{-6p}{h^3}\left(\frac{1}{3}z^3 - \left(\frac{h}{2}\right)^2 z + \frac{z}{3}\left(\frac{h}{2}\right)^3\right) \qquad (18)$$

$$\sigma_{rz} = \frac{-6p}{h^3}\left(\left(\frac{h}{2}\right)^2 - z^2\right)$$

The deflection of the mid plane is

$$w = \frac{P}{64D}\left(\left(a^2 - r^2\right) + \frac{4h^2}{(1-\nu)}\left(a^2 - r^2\right)\right)$$

and the resulting energy stored by the applied stress is

$$G_f = \frac{P^2(1-\nu)\pi}{32Eh^3}\left(a^6 + \frac{6h^2}{1-\nu} a^4\right) \qquad (19)$$

Williams [1: 1683] and others have simplified the far field energy to obtain the energy release rate for a thin

plate by assuming h is much smaller than the radius, a. Applying this assumption, only the term with the a^6 appears on the far field energy and Williams' [1: 1683] calculation for the total energy becomes

$$G_a = \frac{8(1-\nu^2)}{3E} p^2 a^3 \qquad (20)$$

But the total energy, G_a, is the combination of the near and far field energies. Thus, for an interfacial crack between a rigid substrate and an elastic plate the strain energy was found by Andrews and Stevenson [1: 1684] to be

$$G_a = \frac{p^2 a (1-\nu^2)}{2E} \left\{ \frac{3}{32} \left\{ \left(\frac{a}{h}\right)^3 + \frac{a}{h} \frac{4}{(1-\nu)} \right\} + \frac{2}{\pi} \right\} \qquad (21)$$

This equation should give a better representation of the fracture energy for the adhesive plate when it is deflected in the blister test. Most of the data from the previous experiments has fallen between the full stress field solution given by Equation 21 and the modification given by Williams and others in Equation 20.

The approach used by Gent to find the fracture energy differs significantly from Williams, Andrews and Dannenberg. The later used a thick adhesive layer and a small blister radius. Gent [5: 5] assumes the adhesive layer acts like an elastic membrane and the blister is much larger than the adhesive thickness. In addition, he assumes that biaxial

stretching rather than bending is the primary mode of deformation of the adhesive layer. The resulting fracture energies from Gent's equations are:

$$G_a = 0.65\ P_{cr}\ h \qquad (22)$$

$$G_a = 0.39\ (P_{cr}^{\ 4}\ a^4 / E\ t)^{1/3} \qquad (23)$$

Gent's results also showed that the pressure for debond decreased continuously as the blister radius increased. Equation 22 gives a mean value of the fracture energy just using the height of the blister and the critical pressure at debond [6:10]. Equation 23 uses the material properties of the specimen and uses the critical pressure and debond radius.

In the blister test both plate and membrane assumptions are used to determine the adhesive fracture energy. If the deflection of the adhesive layer is small, then the equations for G_a from Timoshenko and from Andrews and Stevenson should provide a better representation. If the deflections are large, then Gent's membrane equations can be used.

II. Description of Test Apparatus

Curing Molds

The curing molds designed were to handle a variety of substrate and adhesive thicknesses up to 3.00 inches. The molds were made of aluminum for low cost and ease of manufacturing, plus aluminum does not interact with the specimens when curing at the low temperatures required for the adhesive, at or below 70° C. A bolt hole was drilled in each corner of the mold so the mold could be leveled thus giving a uniform thickness in the adhesive. The molds were fabricated in four sizes to handle specimens of 1.00", 2.00", and 3.00" diameters and a 3.00" square specimen. A hole was drilled in the bottom of each mold for two reasons. The first was it helped to let trapped air escape when using the vacuum oven so it would not become entrapped in the adhesive layer. Secondly, the hole provided a way to ease the specimens out of the mold after curing. A small bar was used to remove the specimens from the mold by pushing them out from the bottom of the mold. Diagrams of the molds are shown in Figure 2.

Specimens

Two different substrates were used in the blister test. For the initial analysis a plexiglass substrate was used and

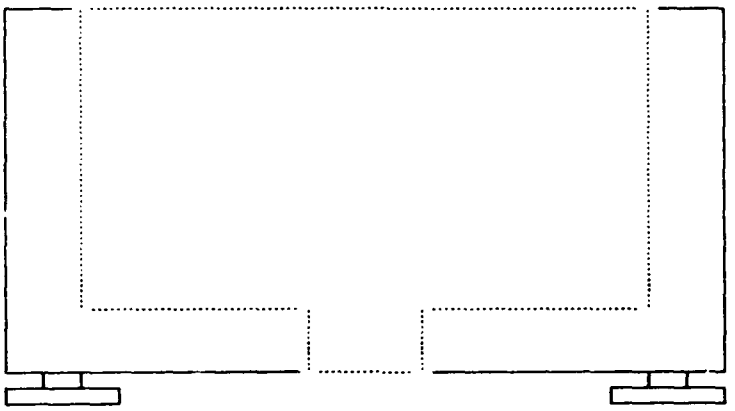

Side View

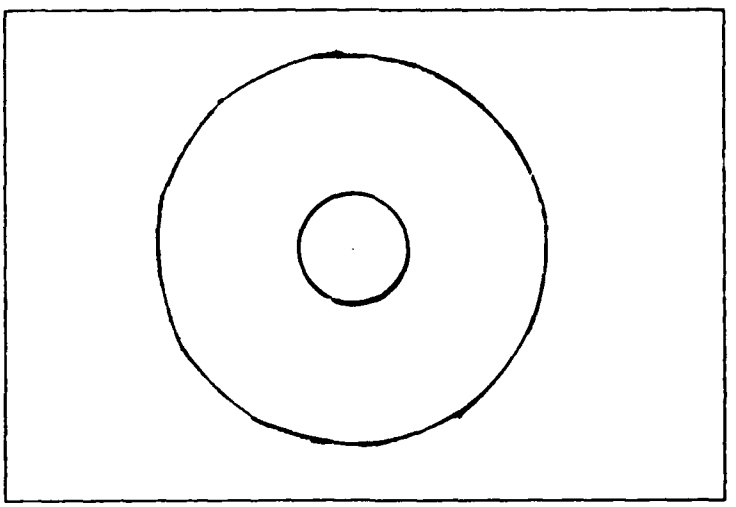

Top View

Figure 2. Specimen Curing Mold

later sodium chloride crystals were employed. Plexiglass was used to: reduce the cost of actually using a crystalline material; to develop a consistent reproducible method of forming the thin adhesive layer on a reusable surface; and to act as a baseline to measure from, since previous experiments had tested a plexiglass substrate. The substrates had holes drilled through the center of each one. The hole radius was one-eighth of an inch. The thicker square plexiglass substrates had an additional hole drilled in their sides to fit the pressure transducer. Clear plexiglass was used so the blister could be observed more easily. Examples of the substrates can be seen in Figure 3. The sodium chloride crystals were unpolished with a surface roughness of $\pm$ 0.020 inches.

The adhesive in the blister test was Arco Hydroxy-terminated Polybutadiene, R-45, and Hexane Triol, HT, with a stoichiometry of ten grams of R-45 to 0.26 grams of HT. It had to be cured for 24 hours at 140 to 160° F. Theoretically there was one isocyanate reactive group for every hydroxyl group in the adhesive. Air Force Astronautics Laboratory, AFAL/MKPB, at Edwards AFB, CA, provided the adhesives.

Young's modulus, E, for the adhesive was found experimentally by AFAL/MKPB. The temperature was varied and E was found for the maximum stress and at rupture, if it occurred, for a dogbone tensile test. The values for E

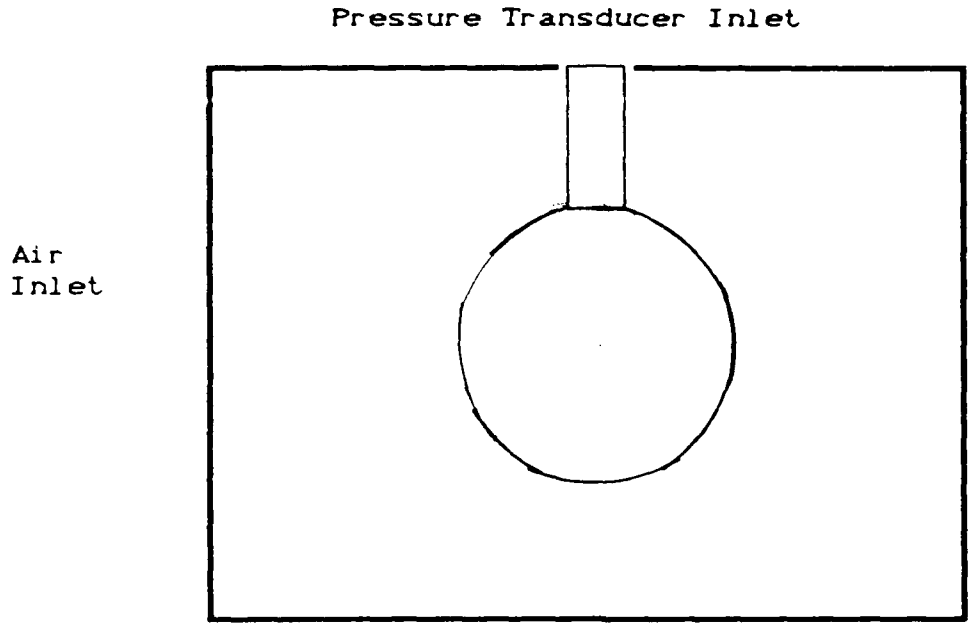

a. Square Specimen Top View

Air Inlet

b. Square Specimen Side View

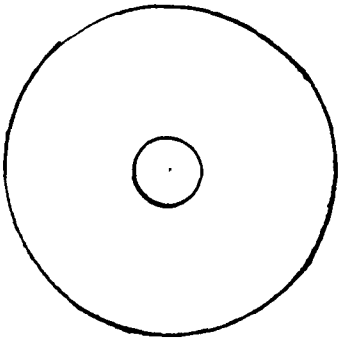

c. Circular Specimen Top View

Figure 3. Plexiglass and Sodium Chloride Specimens

varied from 140 to 180 psi for a temperature of 77^{o} F [6: 2-4], the same temperature the blister test is conducted at . This was the Young's modulus for an adhesive made with Arco, R-45M, and Diphenyl Metnylene Disiocyanate, MDI. This same value was assumed for the R-45 and HT adhesive. The adhesive was assumed to be rubbery at the test temperatures, therefore a typical Poisson's ratio, ν, equal to 0.5 was used in calculating the adhesive fracture energy. Dr. Heidi L. Schreuder-Stacer, AFAL/MKPB, confirmed this value [15]. If testing is done at a different temperature or strain rate the values for E and ν could change.

After removing the specimen from the mold a traveling microscope, with an accuracy of $\pm$ 0.001 inches, was used to measure the adhesive thickness along the specimen's outer edge. An average of the thickness was then used in the calculation of the debond energy. Following the blister test the adhesive film is removed from the substrate and cut in half so the thickness may be examined at the center of the adhesive to account for any error in using the average thickness value.

Data Measurement

The pressure applied to the adhesive, to form the blister and cause debonding, came from a low pressure air source of 80 $\pm$ 0.04 pounds per square inch, (psi). From the main source the air went through a regulator to control the

actual amount of pressure on the specimen. The regulator was rated from zero to three hundred psi in case there was a need to go to a higher air pressure source to reach critical pressure. The air provided a uniform constant pressure across the area of debond so the equations discussed in Section I can be used to calculate work and energy required to debond the adhesive.

The pressure was determined by a pressure transducer. The transducer was either mounted in the square plexiglass substrate or in the plate with the attached air hose line from the regulator for the other specimens. The transducer's rating was 5.35 mV/psi, but calibration of the transducer determined a value of only 5.3188 mV/psi or 0.1880 psi/mV. The transducer was wired to a voltmeter and a storage oscilloscope. The voltmeter provided a visual measure of the rise in pressure and the oscilloscope saved the pressure data plus the corresponding blister height data as a function of time for later comparison to the theoretical models.

Due to the assumptions made and the modeling employed the maximum height of the blister will be at its center. Under the uniform pressure applied from the air source this should be at the center of the substrate debond region where the air inlet hole was located. A linear variable differential transformer (LVDT) measured the displacement of the adhesive at this point. The LVDT is an electromagnetic device that produces a voltage proportional to the

displacement of a movable ferromagnetic core. Its phase is positive or negative depending on which side of the null position the core is moved [8:2]. A twelve inch long plexiglass rod was attached to the movable core so a camera may be used later to record the change in area of the blister per unit of time. A guide plate kept the LVDT centered on the specimen during the test.

The LVDT was not linear throughout its entire range of core displacement. Therefore, the LVDT was calibrated, with the plexiglass rod and guide plate in place,to find this area as shown in Figures 4 and 5. Figure 4 shows the range over which the LVDT was calibrated. Figure 5 marks the most linear section of this data. The lowest value of the linear range, 2.350 Volts, was the minimum value required on the LVDT to begin the blister test. This ensured the displacement was proportional to the voltage. The LVDT was calibrated within $\pm$ 0.001 inch.

The LVDT's output voltage went to a voltmeter and then to a storage oscilloscope where it was stored for data reduction. The transformation used to determine the displacement of the blister was 0.089473 inches per volt. The LVDT's output was a function of temperature, as well as frequency. However, since the blister test was conducted at approximately 25° C (77°F) the change in temperature could be neglected in the computation of the voltage output. The temperature correction factors fell in the range of 10^{-4} to

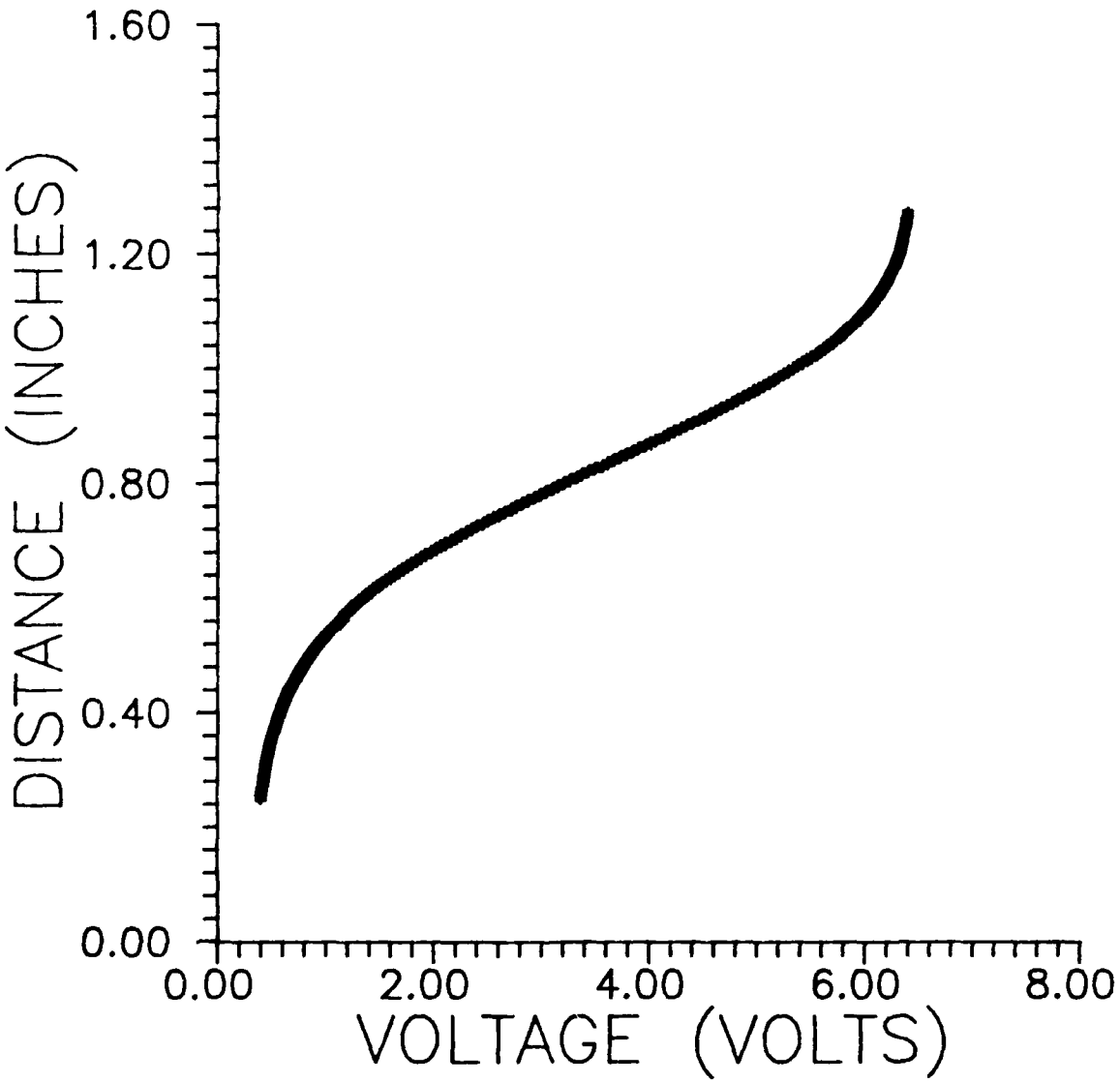

Figure 4. LVDT Calibration Range

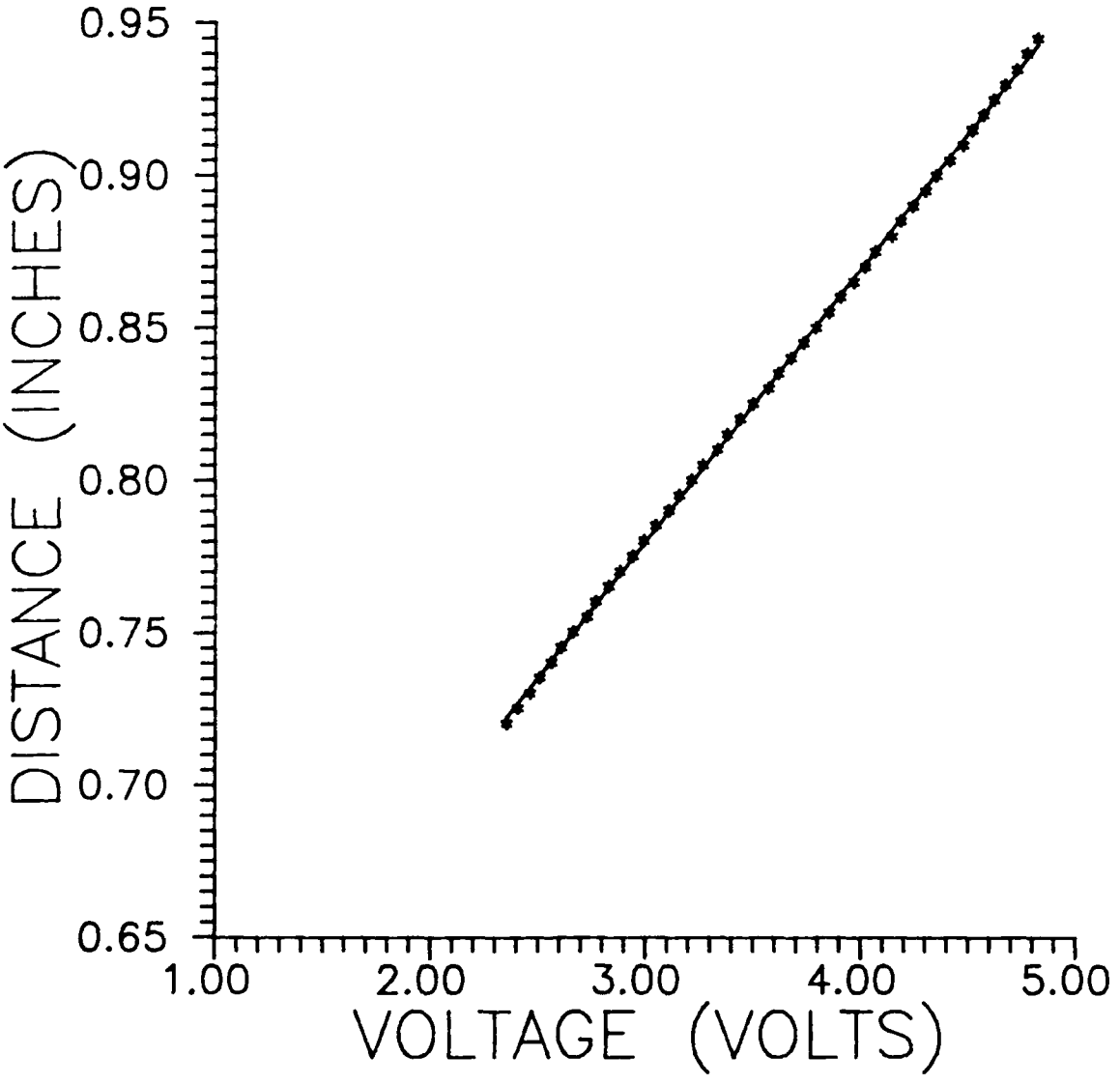

Figure 5. Linear LVDT Range

10^{-7} [8:30] and were only significant for temperatures above 350° C.

The displacement of the LVDT at the center of the blister could only be used accurately if a circular growth of the blister occurred. If the placement of the probe was slightly off-center or the blister did not grow concentrically, the LVDT would be recording a value less than the maximum. This deviation was not significant if plate assumptions were used and displacement was proportional to the pressure. However, when membrane assumptions were applied and the displacement cubed is proportional to the pressure the resulting error could become quite large in calculating G_a.

To account for this equipment set up error the displacement equation was examined:

$$w(r) = \frac{P}{64D}(a^2 - r^2)^2 \qquad (19)$$

Arbitrary values for the blister radius, a, were selected. The displacement of the LVDT away from the center of the blister, r, was examined and the ratios of r/a and w(r)/ w(o) were compared. These calculations are shown in Table 1. If the LVDT was centered within r equal to 0.16a of the blister's center the data would provide at least 95% of the maximum height value. This was accepted because the test period was only 102.3 seconds and the LVDT was recentered

Table 1. LVDT Correction

Blister radius a	r	$w(r)_2 = f(a^2 - r^2)$	w(r)/w(0) %	r/a %
0.03125	0.0000	9.537 E-7	100.0	0.0
	0.0001	9.536 E-7	99.9	0.32
	0.001	9.517 E-7	99.8	3.2
	0.01	7.684 E-7	80.6	32.0
	0.025	1.236 E-7	13.0	80.0
	0.03125	0.0	0.0	100.0
0.0625	0.0	1.526 E-5	100.0	0.0
	0.01	1.449 E-5	94.9	16.0
	0.025	1.077 E-5	70.6	40.0
	0.05	1.977 E-6	13.0	
	0.0625	0.0	0.0	100.0
0.230	0.0	2.798 E-3	100.0	0.0
	0.01	2.788 E-3	99.6	4.3
	0.15	9.242 E-4	33.0	65.0
	0.20	1.664 E-4	5.9	87.0
	0.23	0.0	0.0	100.0
0.330	0.0	1.186 E-2	100.0	0.0
	0.01	1.184 E-2	99.8	3.0
	0.15	7.465 E-3	62.9	45.0
	0.20	4.747 E-3	40.0	61.0
	0.25	2.153 E-3	18.2	76.0
	0.30	3.572 E-4	3.0	91.0
	0.330	0.0	0.0	100.0

r is the position from the center of the blister to the edge of the blister.

before the next test. To be within 99% of the maximum value of deflection the LVDT had to be centered within r equal to 0.065a of the actual blister center. As the radius of the blister increased this error decreased. The reason was: if the blister grew concentrically the a^2 term would increase and the placement of the LVDT at r would not increase, and the ratio of r/a would approach the value of 0.16.

The output voltage for the pressure transducer and LVDT were sent to channels X and Y on a storage oscilloscope. The oscilloscope provided a temporary record of the changes in pressure and height for each blister test. Once debond had occurred and the adhesive had vented the pressure to the atmosphere, the data could be examined on the oscilloscope. From the oscilloscope the data was down loaded via a computer program to a floppy disk, thus providing a permanent record. This procedure was repeated for each blister test.

There were some limitations with the storage oscilloscope. The first was the memory which was limited to a maximum storage capacity of 102.3 seconds. Over this period 1023 bits of data were stored. This means there were ten samples per second of the voltage taken during the test. Actual blister tests lasted longer than this time interval when the critical pressure needed was large. So, after each test of 102.3 seconds the pressure was reduced on the specimen, the height and pressure voltages in the oscilloscope's memory sent to a computer disk to be stored,

the LVDT reset and the blister test restarted.

The second limitation was the trigger mechanism on the oscilloscope. Because the voltage was so low, in the millivolt range, the magnitude of the change in the pressure voltage was too small to consistently trigger the oscilloscope and automatically begin taking the data. Because of this, the oscilloscope was triggered manually and then the air pressure was increased. The time at which the oscilloscope was triggered was also monitored to ensure the blister test did not exceed the maximum storage capacity of the oscilloscope. The computer program that transferred the data was GURU by Tektronix, Inc.

III. Test Procedure

Cure Process

There were two main steps in the formation of the thin adhesive film onto the substrate. First was the preparation of the substrate and secondly was the preparation of the adhesive. Both are discussed below along with some problems encountered in the forming of the adhesive on the substrate.

The substrate was prepared by first plugging the center hole with a metal pin coated in teflon tape. The pin was mounted flush with the surface where the adhesive would be applied. The pin stuck out, 0.25 inches, from the bottom surface so it could be removed from the substrate after curing.

Next, silicone vacuum grease was spread on the substrate's sides. This was so the substrate could be removed easily from its mold following curing, and it kept any of the adhesive from slipping between the mold and the substrate, thus bonding them together. Then a very small amount of silicone grease was placed around the center hole, radius of about 7/32 inch, on the top surface. The silicone around the center hole prevented the adhesive from forming near the center hole and acted as the initial debond between the substrate and the adhesive.

The adhesive was prepared by first weighing the epoxy.

The epoxy used to develop the proper casting techniques was Hydroxy-terminated polybutadiene, R-45. Ten grams of R-45 was mixed with 0.26 grams of the reacting agent. This material is similar to the elastomer matrix used in solid rocket fuel. After weighing, the epoxy was preheated at a temperature of 50^{0} C and de-gassed at -25 inches HG in a vacuum oven. The reacting agent, Hexane Triol (HT), was then mixed with the epoxy and placed back in the vacuum oven. After two minutes the adhesive was remixed and placed back in the oven for five more minutes. This step was repeated one more time. The adhesive was then poured into the mold onto the substrate. The mold was finally placed in the oven to cure. After twenty-four hours the heat was turned off and the oven vented so the specimen could gradually cool to room temperature, thus avoiding thermal shock.

The vacuum oven was used to remove small air bubbles and any moisture from the adhesive. Dr. Schreuder-Stacer, AFAL/MKPB [14], said the humidity makes a significant difference in the curing process. The actual rocket fuel has problems with air pockets due to the changes in temperature and humidity in the storage, weighing, mixing, and curing of the fuel. By attempting to keep the adhesive free from humidity and the temperature relatively constant some of these factors could be minimized. By reducing the amount of silicone grease placed on the substrate the larger surface air bubbles were removed. There were still a few small air

bubbles occasionally in the adhesive, located around the center air inlet hole and on the edge of the specimen. Dr. Schreuder-Stacer examined the specimens and explained that the air pockets were caused by the moisture in the silicone grease. The evaporation of this moisture formed the air bubbles. Not all of this air could make its way through the adhesive layer before the adhesive started to cure.

Dr. Schreuder-Stacer recommended the following steps to remove the remainder of the air bubbles in the specimen [15]:

1) Use teflon tape in the mold instead of silicone grease.

2) Use teflon tape instead of silicone grease over the center hole of the specimen. This tape has adhesive on one side to keep it in place on the crystal substrate, then the adhesive is added.

3) Prepare the crystals by using a three-step process:

   a) In both a clockwise and anti-clockwise motion wipe the crystal on a water dampened cloth.

   b) Repeat this process on an acetone dampened cloth.

   c) Repeat this process on a dry cloth.

   Continue these steps as necessary to polish down the ridges on the sodium chloride crystal. Be careful not to dissolve the crystal or to polish it unevenly.

The first eleven blister tests were done on unpolished, as received crystals. The remaining crystal tests used polished specimens. It is assumed that the fracture energy

would be higher for these specimens than the previous crystal specimens, since there should not be a preferred direction and stress concentration effect, along the ridge lines, for the adhesive to fracture and debond along.

Blister Test

The blister test equipment was set up as in Figure 6. The pressure to debond the adhesive from the substrate came from a low pressure air source of 60 psi. When the air was turned on the regulator controlled the amount of air into the specimen. The data for the pressure and height were recorded on the storage oscilloscope and also monitored on the voltmeters, as discussed in Section II.

As the pressure was gradually increased the height of the blister increased proportionately while its initial radius, a_o, remained constant. This was the elastic region where the blister deflection represented either a plate or a membrane. The deflections of a plate are proportional to the applied pressure and for a membrane its deflection should be proportional to the cube root of the applied pressure according to Gent [5:5].

Due to the memory capacity of the oscilloscope, i.e. a maximum storage of 102.3 seconds, the test was conducted over this time interval. The time was closely monitored so if

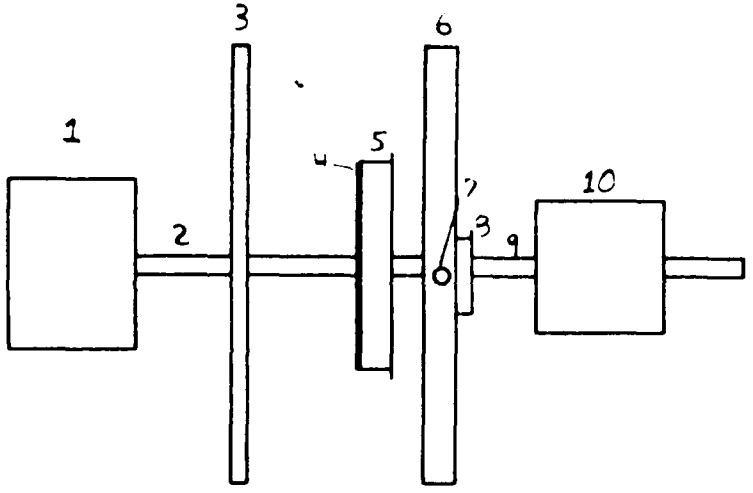

1. LVDT
2. Plexiglass rod
3. Guide Plate
4. Adhesive layer
5. Substrate
6. Specimen holder
7. Pressure Transducer
8. Brass fitting
9. Air hose
10. Regulator

Figure 6. Blister Test Set-up

critical pressure appeared to be reached near the end of the test period the pressure was reduced and then the next test started at a pressure slightly less than the maximum of the previous test.

The outline of the blister was marked on the specimen so its growth could be tracked visually. The blister radius was measured with a 1/64 inch increment ruler. This data was recorded by the test operator and written as a function of the LVDT voltage. When the blister radius grew the LVDT voltage was annotated so the exact time of debond could be determined on the oscilloscope data.

If the adhesive film was made too thin the blister test failed due to cohesive failure and rupture in the adhesive, rather than between the substrate and the adhesive. When the adhesive layer was too thin due to air bubbles a thin layer of epoxy was placed in a circle around the center of the adhesive layer. Dannenberg [5: 128] had used varnish in his blister tests for the same reason, to avoid cohesive failure. Dannenberg [5: 131-132] discovered that it was the first layer of the adhesive that had the greatest effect on the fracture energy, and that varying the total thickness of the adhesive had not as much of an effect on fracture energy. When the epoxy was used the initial fracture energy was not examined until the blister radius was greater than the epoxy radius. In addition the thickness effects of the epoxy were removed by zeroing the LVDT before testing. Appendices A and

B contain a list of the equipment used and a detailed test procedure. The high speed camera was not used because the lighting required for a clear picture raised the temperature of the specimen by 100^{O} F.

IV. Experimental Results

Cured Specimen

Average values for specimen geometry and material properties were used in energy calculations. The thickness of the adhesive was based on an average of measurements taken along the specimen's outer edges. The material constants: Young's modulus and Poisson's ratio, were assumed average values for the test temperature of 77^{O} F. Young's modulus was found experimentally, by AFAL/MKPB [8: 3-5], in a dogbone stress test for the adhesive made with R-45M and MDI. The values of E ranged from 140 to 180 psi at a temperature of 77^{O} F depending on the strain rate applied. An average value of E equal to 160 psi was used in the calculation of fracture energy. The adhesive was assumed to be rubbery and ν equal to 0.5 was used in all equations to compute fracture energy. This was the same value assumed by Hencky , Gent and others [6: 14] for an incompressible elastic layer. It was a good value for this adhesive at these test conditions according to Dr. Schreuder-Stacer [15].

The stoichiometry of the specimens was not exactly the same every time due to many factors including: the mixing of the materials, humidity of the air, variances in weight and volume of the chemicals, as well as the amount of chemicals de-gassed in the vacuum oven. These factors could create

some air bubbles and voids in the material.

The final specimens produced during the test showed a remarkable improvement over the first specimens. The air bubbles first observed in the cured specimens have been reduced, if not eliminated, using the vacuum oven and limiting the amount of silicone grease applied over the center of the specimen. The thickness of the specimen was increased from 0.0595 to 0.1366 $\pm$ 0.015 inches to avoid cohesive fracture during the blister test. The substrate used has gone from a simple plexiglass plate to a crystal similar to the actual crystalline particulate oxidizer in the solid rocket fuel under investigation. A simple initial debond area for the specimen was developed using silicone grease and a metal pin to form a constant radius, a_o, for the specimens.

Blister Test Results

The adhesive fracture energy of the adhesive computed by applying Gent's, Timoshenko's, and Andrews and Stevenson's equations are listed in Tables 2, 3 and 4. Some specimens were able to be tested more than once. This was because after the initial debond and growth of the blister the pressure was reduced on the specimen and the test repeated until cohesive failure or complete debond of the the adhesive from the substrate occurred. Appendix C lists the specimen's average thickness, maximum height of the blister, its radius

Table 2. Computed average values of G_a for Adhesive on Plexiglass. (lbf*in/in)

	Specimen #			
	2	3	4	5
Size ± 1/64"	2.00 D	2.00 D	3.00 Sq	2.00 D
Thickness ±.001"	0.0743	0.0735	0.0712	0.0595
G_a 1.	17.931 (5)	1.233	1.259	4.784 (5)
G_a 2.	2.739	0.600	1.118	0.942
G_a 3.	1.980	0.660	1.325	1.293
G_a 4.	10.680	0.808	1.131	2.776

D Diameter
Sq Square
1. Timoshenko's Plate Theory, Equation 15
2. Gent's Membrane Theory, Equation 23
3. Gent's mean value, Equation 22
4. Andrews and Stevenson's Plate, Equation 21
5. Specimen had a non-adhesive failure: blew up like a balloon with no growth in radius but large deflection and deformation of the adhesive.

Table 3. Computed average values of G_a for adhesive on Unpolished Crystal. $(lbf*in/in^2)$

	Specimen #				
	6	8	9	10	11
Size ± 1/64"	1.94 D	1.94 D	3.00 D	1.94 D	3.00 D
Thickness ±.001"	0.0100	0.0900	0.1366	0.0948	0.0796
$\bar{G}_a$ 1.	121.22 (5)	0.054	0.003	0.223	0.051
$\bar{G}_a$ 2.	0.350	0.134	0.045	0.193	0.061
$\bar{G}_a$ 3.	0.185	0.022	0.022	0.901	0.008
$\bar{G}_a$ 4.	60.801	0.048	0.005	0.014	0.031

Table 4. Computed average values of G_a for an adhesive on Polished Crystal $(lbf*in/in^2)$

	Specimen #
	12
Size ± 1/64"	1.94 D
Thickness ±.001"	0.0995
$\bar{G}_a$ 1.	0.006
$\bar{G}_a$ 2.	0.041
$\bar{G}_a$ 3.	0.012
$\bar{G}_a$ 4.	0.006

D Diameter
Sq Square
1. Timoshenko's Plate Theory, Equation 15
2. Gent's Membrane Theory, Equation 23
3. Gent's mean value, Equation 22
4. Andrews and Stevenson's Plate, Equation 21
5. Specimen had a non-adhesive failure: blew up like a balloon with no growth in radius but large deflection and deformation of the adhesive.

and the critical pressure. The fracture energy found in Tables 2, 3 and 4 came from these values. The first substrates were plexiglass and the average values of G_a for each specimen are shown in Table 2. Similarly for the unpolished crystal specimens and the polished crystal in Tables 3 and 4 respectively. These values for G_a were determined by averaging the adhesive fracture energy that occurred at each blister growth. The ranges of each of these values of G_a are shown in Appendix D for each specimen.

From Table 2 specimens 3 and 4 had values of G_a, considering Timoshenko's equation, that were approximately the same. Andrews and Stevenson's value for specimen 4 was similar to those found by Timoshenko. In Table 3 specimen 8 and 11 had similar values for G_a according to Timoshenko and Andrews and Stevenson. Specimen 9 had values similar to the polished crystal in Table 4. These specimens were being examined near the lower end of the recordable data.

There was a large difference between the values of fracture energy found in the blister test. From Timoshenko's plate theory the values ranged from 0.155 to 25.74 $lbf*in/in^2$. The membrane theory by Gent had values from 0.320 to 2.926 $lbf*in/in^2$ for the plexiglass substrate. The crystal specimens had values from 0.001 to 130.199 $lbf*in/in^2$ for Timoshenko's plate. Gent's membrane had values of 0.024 to 0.369 $lbf*in/in^2$.

Disparities arise in these values due to the assumptions

made in their equations. Timoshenko assumed small deflections and plane sections remain plane after deformation. Gent assumed an elastic membrane and a large blister radius to model thin adhesive layers with large radius to thickness ratios of 138 to 417 [6:5]. Both assumed linearly elastic deflections. Timoshenko's solution yielded a deflection due mainly to bending deformation. While Gent's solution was driven by tensile deformation in the membrane. Andrews and Stevenson used a combination of the near and far field energies to combine the fracture energy and the finite internal strain energy.

The plate theory values for the fracture energy were usually much higher than those found by the membrane theory in specimens 2, 5 and 6. This may be accounted for due to the thickness of the adhesive versus the size of the blister which was more like a membrane than a plate and there was a non-adhesive failure occurring in the adhesive. As the pressure and height of the blister increased the deflections in the adhesive no longer could be assumed to be small. Thus, for the larger deflections in the blister, which at times appeared to blow-up like a balloon without any adhesive fracture, the plate theory is not very accurate, and cohesive fracture was occurring. For the smaller deflections, found at the initial adhesive fracture of each specimen, it was still all right to assume a valid plate theory.

Using the membrane theory developed by Gent the values

of fracture energy fell more in the expected range for the adhesive in specimens 2, 5 and 6. The mean values found using just the critical pressure and height of the blister came closer to the fracture energy when examining later debond in the adhesive and not the initial value. The actual value of the fracture energy lies somewhere between these two theories.

Comparing the different equations for fracture energy and their assumptions it was found that the thicker the specimen's adhesive layer the farther apart the membrane and plate theories were from one another, as was expected. For a thickness between 0.0595 and 0.0712 inches the fracture energy found by Gent, Equation 23, and Timoshenko, Equation 15, for the initial debond differed by only 4 percent on a plexiglass specimen. As further debond occurred for the same specimen the mean fracture energy found by Gent, Equation 22, approached within 4 percent of the value for the membrane fracture energy found in Equation 23.

For a thicker adhesive layer, 0.0712 to 0.0735 inches, the fracture energy equation derived by Andrews and Stevenson, Equation 21, approximated both the plate and membrane equations quite well. At the initial debond, when the height and radius of the blister are small and the blister resembles a plate, Andrews and Stevenson's fracture energy was within 1 percent of Timoshenko's. At the second debond of these same specimens the fracture energy was within

6 to 8 percent of Gent's expected values. Another result is that the mean fracture energy for these specimens was within 9 percent of the value found by Timoshenko for the second debond.

After the initial debond, for the same pressure rate in a crystal specimen, the adhesive fracture energy is a constant of $\pm$ 0.0015 Lbf * in/ in^2 according to all of the theories. In the last specimen tested G_a was computed as 0.006 lbf*in/in^2 using plate theory. This does not include the initial debond fracture energy. This crystal had been prepared by polishing with water and acetone to remove any ridges on the adherand surface. The maximum deflection of the adhesive was only 0.15 times the thickness of the adhesive. The maximum radius of debond was 3.45 times that of the thickness. This value is much lower than Gent's [6: 4-5] ratio, 70 to 210, of debond radius to adhesive thickness. Because of this Gent's values for G_a, 0.0405 $\pm$ 0.05 Lbf * in/ in^2, are much higher using the thin membrane approximation to compute the adhesive fracture energy.

For specimen 9 using the same pressure rate G_a was computed to be 0.003 lbf*in/in^2 for Timoshenko's equation and 0.005 lbf*in/in^2 for Andrews and Stevenson's equation. The ratio of radius to adhesive thickness was 2.52 and the ratio of maximum deflection to thickness was 0.084 for this specimen. This shows that the ridges had not been allowing the debond to occur more easily along these preferred lines

because there was not that much of a change in G_a.

The adhesive fracture energy was affected by the pressure rate. The higher the pressure rate the higher the computed value of G_a. This agrees with Andrews and Stevenson's results. And when a constant rate was applied to a specimen the G_a assumed a constant value. For a rate of 0.0150 $\pm$ 0.003 psi/sec G_a equals 0.0055 $\pm$ 0.0015 lbf*in/in^2 for the polished specimen and for an unpolished specimen. These are based on the adhesive layer behaving as a plate rather than a membrane during the experiment. At a rate of 0.0254 $\pm$ 0.003 psi/sec the adhesive fracture energy equals 0.0073 $\pm$ 0.0018 lbf*in/in^2 for an unpolished specimen using the plate approximation. The values obtained in previous blister tests used a much higher pressure rate, 10 to 10^6 psi/sec [1: 1681]. The values obtained for G_a in these tests were 0.571 to 1.142 lbf*in/in^2. At a comparable pressure rate it is expected that G_a for this specimen will also increase to these values.

The mean values of adhesive fracture energy for the different substrates are shown in Table 5. The initial fracture energy of each specimen has been disregarded and the adhesive layer is examined as a plate.

The plexiglass substrate had the largest values of G_a. Considering the large deviation, up to one-third of the mean value, these values fall within a value of 1.00 lbf*in/in^2. On the unpolished crystal the values of G_a were the lowest

Table 5. Mean Values of G_a on Different Substrates

($lbf*in/in^2$)

Plexiglass	Unpolished Crystal	Polished Crystal
1.246±.013	0.091±.056	0.006±.001 (1)
0.859±.259	0.108±.063	0.041±.001 (2)
0.993±.333	0.238±.216	0.012±.001 (3)
0.970±.162	0.037±.023	0.006±.001 (4)

1. Timoshenko's Plate Theory, Equation 15
2. Gent's Membrane Theory, Equation 23
3. Gent's mean value, Equation 22
4. Andrews and Stevenson's Plate, Equation 21

using a plate approximation, and had less deviation than if a membrane approximation was used. But these values of G_a had the largest deviation from the mean value. The deviations in these values of G_a are over half the mean value, and in the case of Gent's mean theory it is almost equal to the mean value. The polished crystal had the smallest values for G_a with the smallest deviation. The plate theory approximations using Timoshenko's equation and Andrews and Stevenson's equation agreed. The membrane value of G_a was at least twice that of the plate value. The reason for less deviation could be partially due to only one polished crystal was tested and at least five of each of the other substrates were tested. The greater the surface area the more energy was required to cause debond. The plexiglass' surface area was larger than the unpolished crystal's area, which was larger than the

polished crystal's surface area. The unpolished crystal is a better representation of the actual crystalline material being modeled in the solid rocket fuel due to its surface roughness.

Considering Andrews and Stevenson's computed values of G_a, and examining G_a versus a ratio of blister radius to deflection for all the specimens, the adhesive fracture energy could be considered a material property for a certain test range. This is considering only the adhesive fracture of the specimens and disregarding any cohesive fractures when the blister blew-up like a balloon. Plots of this data are shown in Figures 7 and 8 for the plexiglass and unpolished crystal substrates respectively. The horizontal line in the plots is the mean value of G_a. The vertical lines represent the deviation of the test data from the mean. Table 6 lists these mean values and ranges that the blister radius/ deflection ratio (a/h) represents G_a as a material property for this blister test. Table 6 also lists the ranges of radius/ thickness ratio (a/t) and deflection/ thickness ratio (h/t) for which G_a could be considered a material property. Plots similar to those in Figures 7 and 8 for the plexiglass and unpolished crystal substrates showing G_a versus a/t and h/t are in Appendix D.

For the plexiglass substrate the test data below an a/h ratio of 2.5 was too varied to give an accurate reading of G_a as a material property. Ratios greater than 3.5 were not

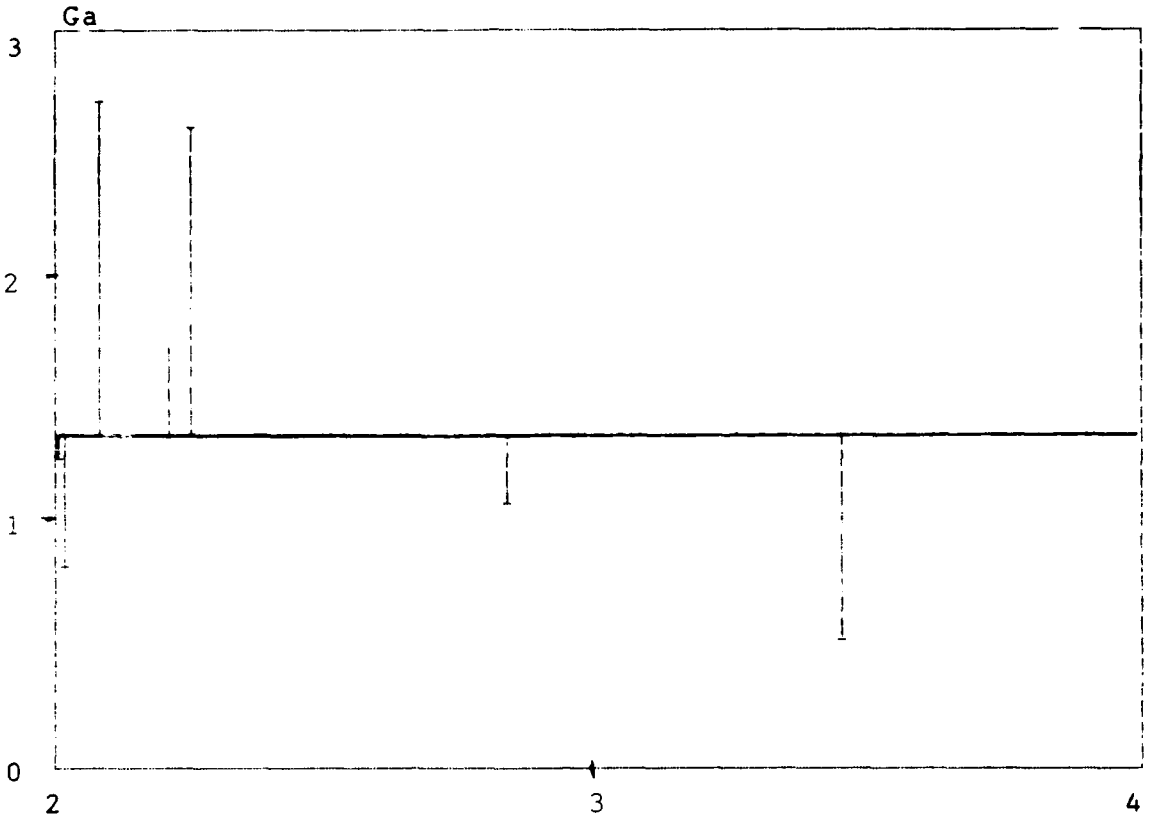

Figure 7. Plot of Adhesive Fracture Energy versus Blister Radius/Deflection Ratio * for all Plexiglass Substrates

* Horizontal line represents the mean value.
Vertical lines represent deviation of the experimental data from the mean value.

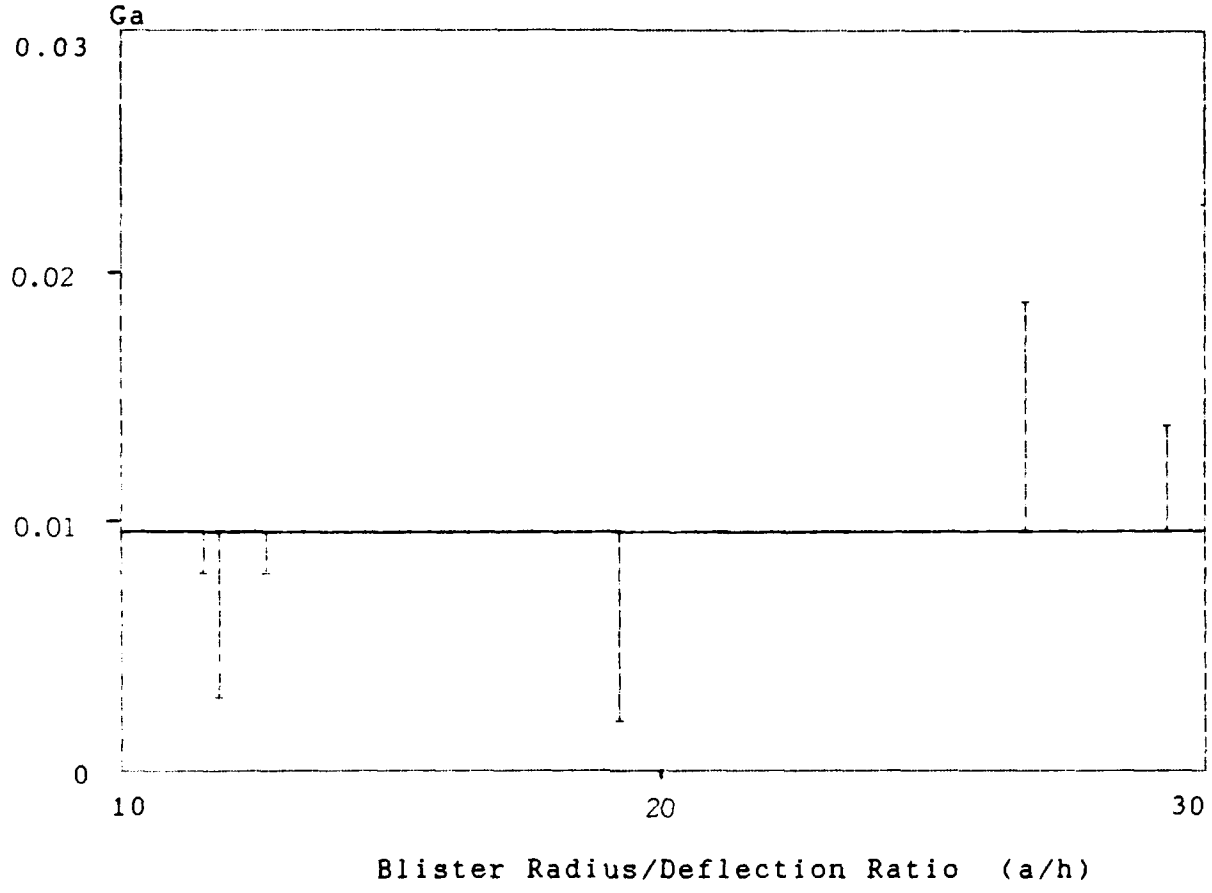

Figure 8. Plot of Adhesive Fracture Energy versus Blister Radius/Deflection Ratio * for all Unpolished Crystal Substrates

* Horizontal line represents the mean value.
Vertical lines represent deviation of experimental data from the mean value.

Table 6. Test Ranges of G_a as a Material Property

Substrate	Mean G_a ($lbf*in/in^2$)	a/h Range	a/t Range	h/t Range
Plexiglass	1.341	2.0 to 3.5	3.5 to 4.0, and 6.0 to 8.0	1.8 to 3.5
Unpolished Crystal	0.010	10 to 16, and 24 to 30	1.7 to 5.0	0.10 to 0.25
Polished Crystal	0.006	49 to 80	2.5 to 3.5	0.14 to 0.15

examined. In the unpolished crystal substrates the two ranges of a/h listed in Table 6 could represent G_a as a material property. In between these ranges the test data was not conclusive enough to state G_a was a material property. The polished crystal had only two test points and the range of a/h that G_a could be a material property is listed in Table 6. More test data is required to determine if there is a ratio of a/h, outside of the stated regions, where G_a is not a material property. Similarly for the ranges of a/t and h/t. As the h/t ranges suggest, the deflection for the crystal substrates were less than the thickness of the adhesive. The plate model did give the best results and was

in agreement with Malyshev and Salganik's results [3: 33, 36].

Deflections of the plate are directly proportional to the pressure and in the membrane the deflections are proportional to the cubed root of the pressure. As was observed during the blister test experiment the adhesive acted as a plate for small pressures. Some examples of this relationship are shown in Figures 9 and 10. Additional test results are shown in Appendix D. The test data is shown as the starred points. The area between the upper solid lines represents a clamped Timoshenko plate boundary condition for the given test data and possible data variation. The area between the dashed lines represents the clamped Andrews and Stevenson plate for the same conditions. The lower solid line represents a simply supported Timoshenko plate for the given conditions. Variation of this data is not shown since the experimental data did not represent this mathematical model. The test data falls closest to the Andrews and Stevenson clamped plate conditions. The specimens in these figures were a 2.00 inch diameter and a 3.00 inch square plexiglass substrate. The blister radius in Figure 9 was 23/128 inches and in Figure 10 was 17/64 inches. The blister radius was constant until adhesive fracture occurred at the last data point, p_{cr}. The curves do not show a cubic relationship between the pressure and deflection as Gent's [6: 3] membrane theory suggests. Roughness in the data is due in part to variations in the

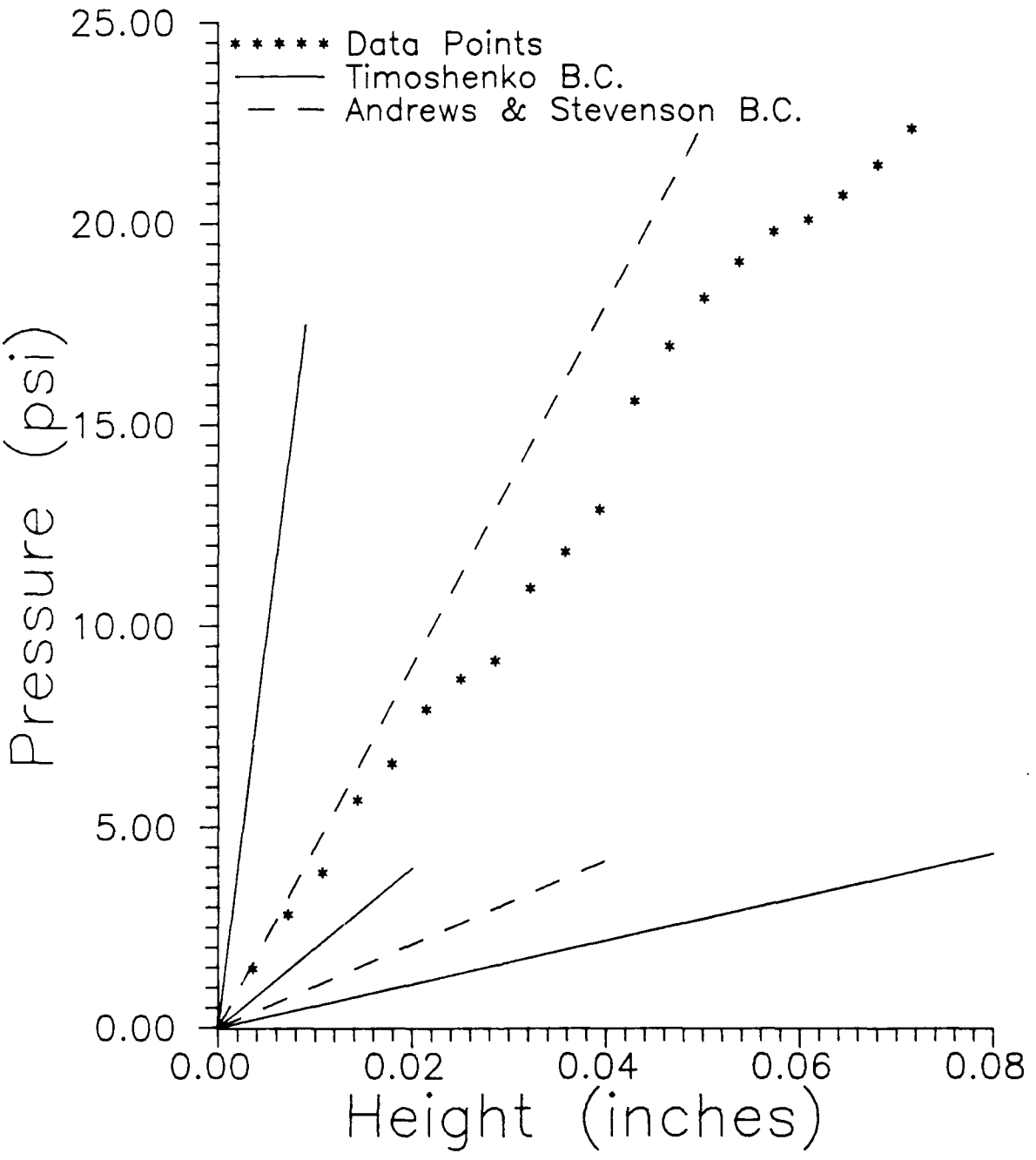

Figure 9. Blister Pressure versus Height until Adhesive Fracture Specimen No. 2. Test Date 23 Sep 88.

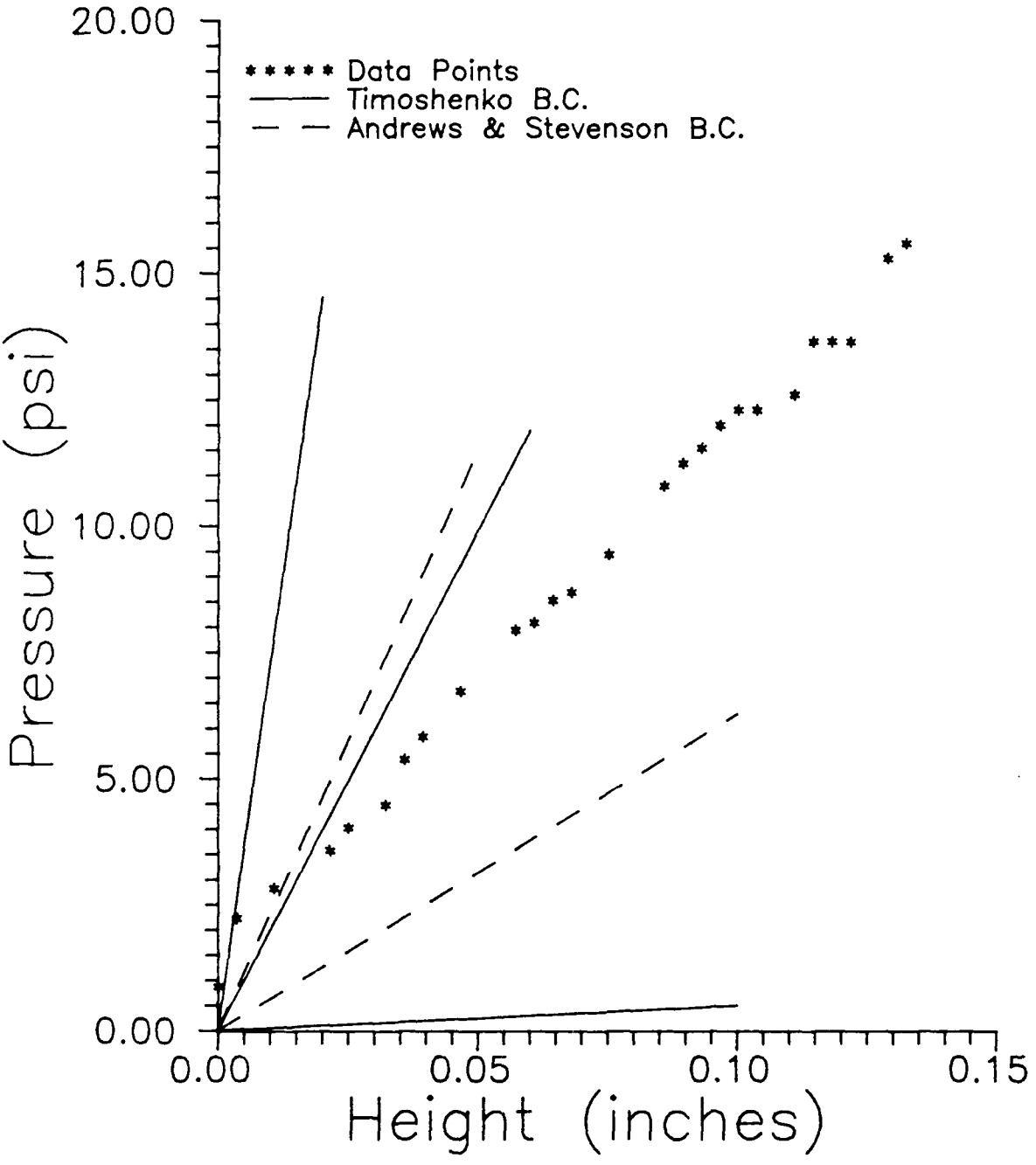

Figure 10. Blister Pressure versus Height until Adhesive Fracture Specimen No. 4. Test Date 28 Sep 88.

pressure flow, $\pm$ 0.04 psi. The best correlation with basic plate theory resulted for deflections less than the thickness of the adhesive in accordance with Malyshev and Salganik's results [3: 33,36]. In these curves the blister radius was constant during the increase in pressure.

In some of the plexiglass specimens a slightly non-linear relation was found. This is shown in Figure 11 for a 2.00 inch diameter plexiglass substrate with a blister radius of 39/128 inches. This figure is a plot of the change in pressure versus the change in height. the initial point was based on a prior linear test. This test was started at a higher pressure since the previous test on this specimen showed no change in blister radius for the lower pressure. Any change in height from a zero load condition until the initial test load was accounted for by: (1) zeroing out the LVDT prior to recording the new test data (2) adding the initial deflection to the change in deflection reached at debond and (3) adding the initial pressure to the change in pressure to compute G_a. The pressure versus deflection is linear up to the point where large deflections in the adhesive began to occur for a small change in pressure. Here the adhesive may best be represented by a polynomial equation of the second and third order respectively. The equation for Figure 11 is: $Y = 485\ X^2 + 1$. The coefficients associated with the squared and single value terms are not that small. This specimen has extra rigidity and is not within the plate

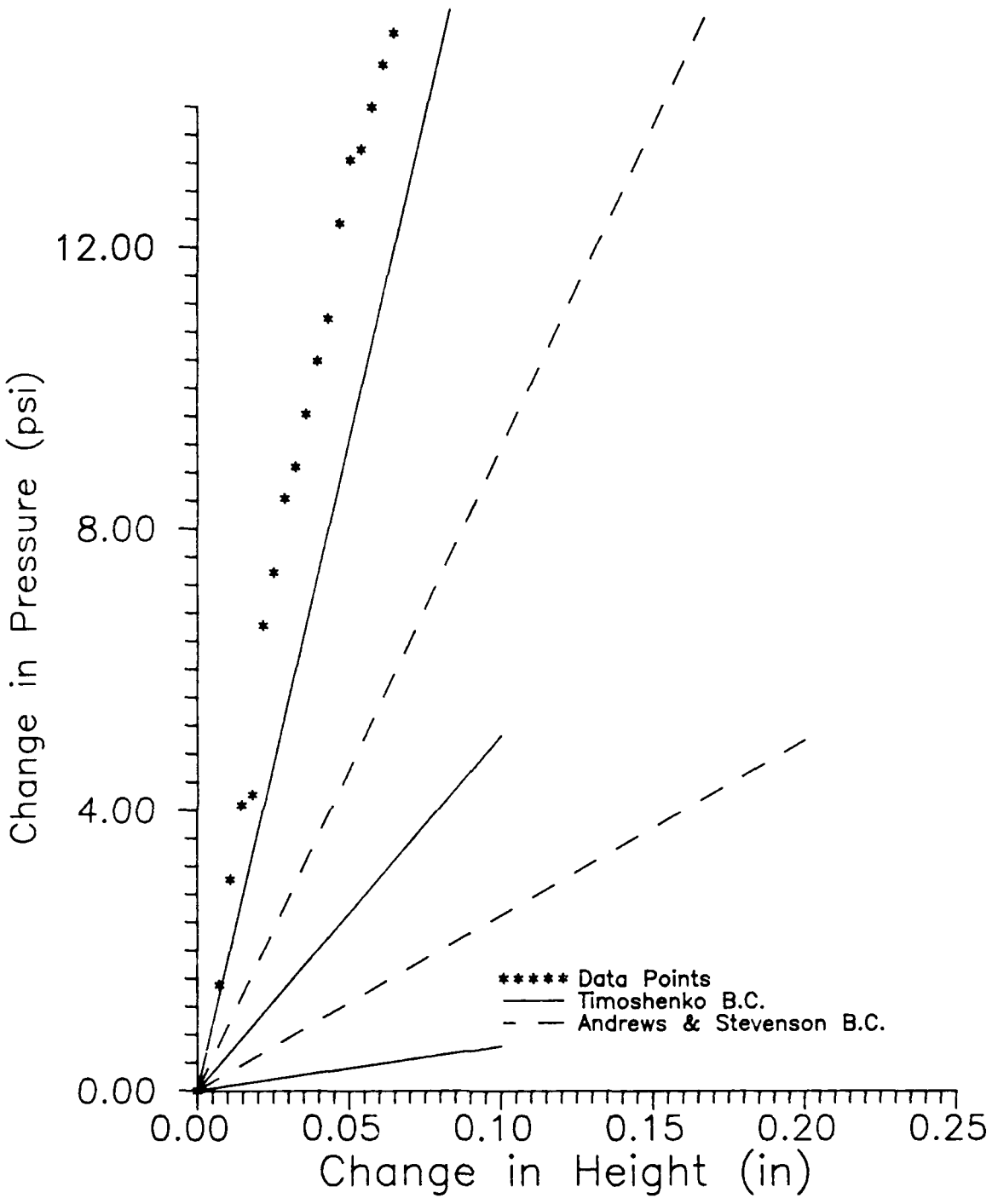

Figure 11. Blister Pressure versus Height until Adhesive Fracture Specimen No. 2. Test Date 23 Sep 88.

theory. The radius versus thickness does not represent a plate model and the specimen was undergoing a non-adhesive fracture. Thus, for the crystal specimens which only had small deflections, the calculation of G_a using the plate theory best approximates the experimental data.

The blister test developed has given consistent repeatable data. Figure 12 shows that adhesive fracture energy was a function of debond pressure and specimen geometry. The dimensionless values of adhesive fracture energy for the specimens versus the ratio of thicknesses to radii of the blister are shown in the figure. Deviations in pressure, adhesive thickness and blister radius are also plotted for each of these points. This data falls approximately on the theoretical values for the Andrews and Stevenson plate. These theoretical values are shown by the dashed line . For thickness to radius ratios less than 0.5 this data was comparable to that found by Andrews and Stevenson [1 :1686] and Bennett, De Vries and Williams [3: 40].

The same dimensionless plot for specimen number 12 is shown in Figure 13. This crystal specimen's surface was washed with water and acetone to remove any ridge lines and surface imperfections. This data shows that the adhesive fracture energy has leveled off and assumed a constant value. An increase in the thickness to radius ratio should not change this value.

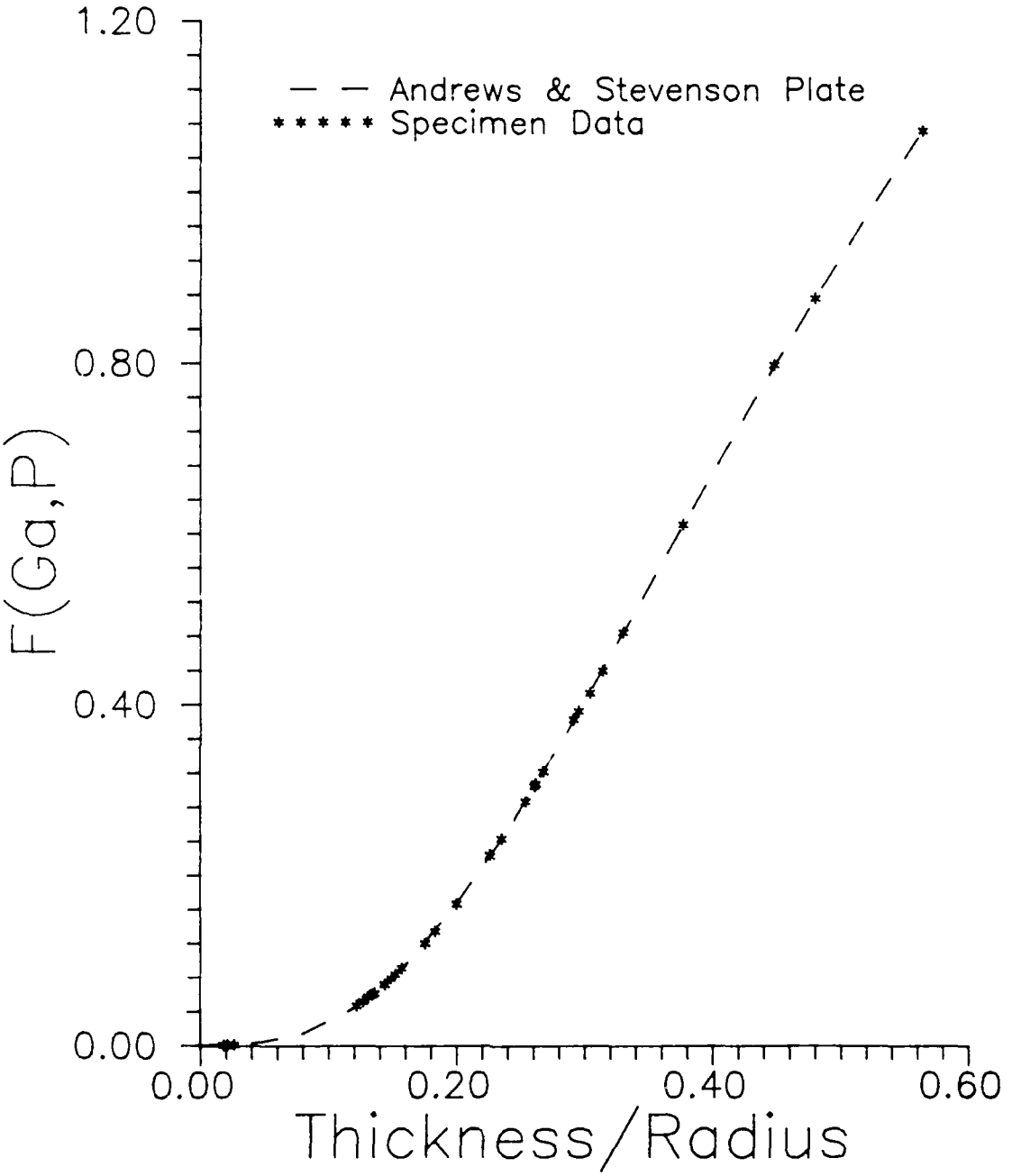

Figure 12. Non-dimensionalized Plot of Adhesive Fracture Energy
F(Ga,P)= Pressure^2 * Radius/(E*Ga)
Specimen No. 1 to 11

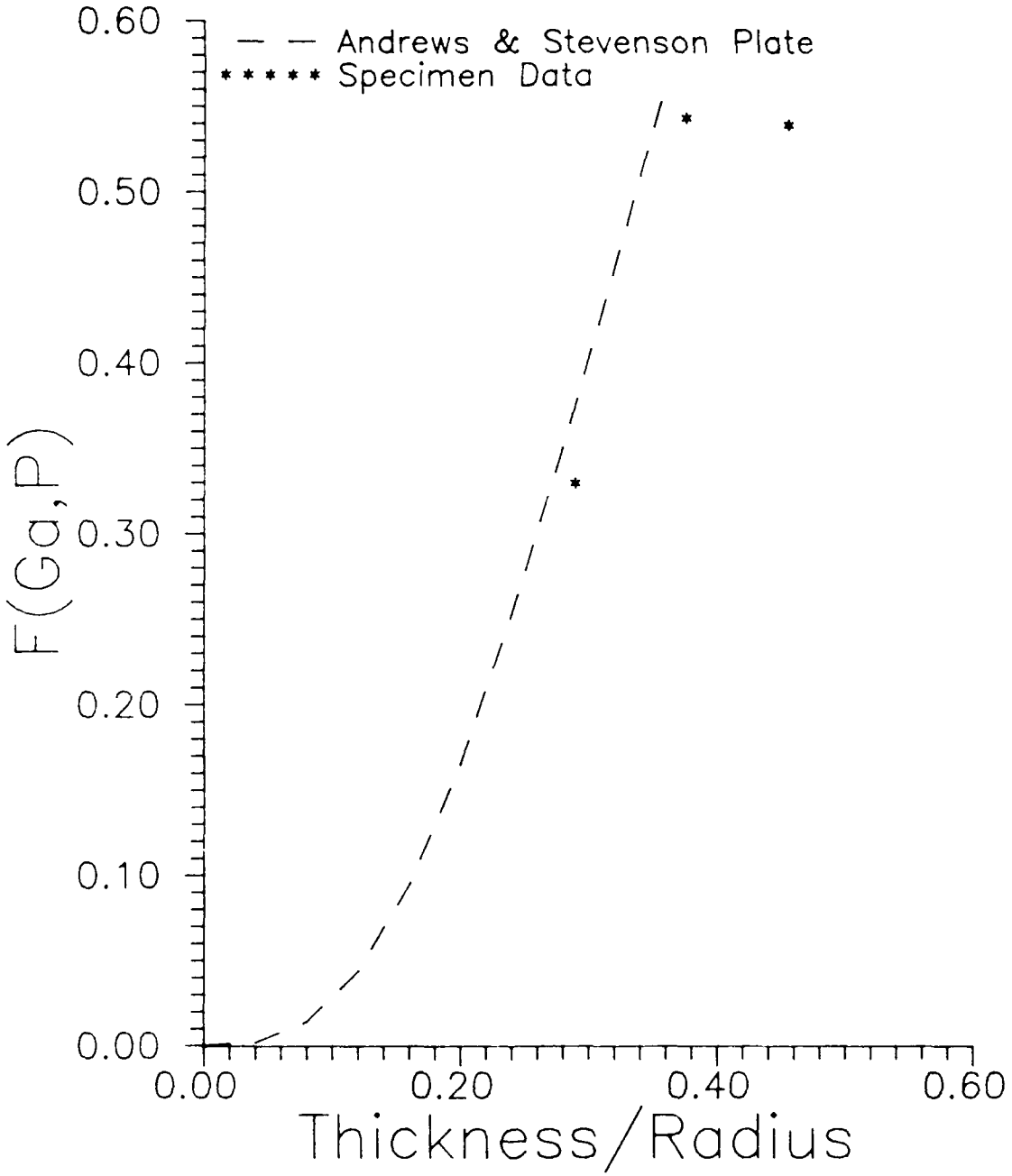

Figure 13. Non-dimensionalized Plot of Adhesive Fracture Energy
$F(Ga,P) = Pressure^2 * Radius/(E*Ga)$
Specimen No. 12

Examining the values of adhesive fracture energy in the crystal specimen versus the blister radius is shown in Figure 14 for specimen 12. After initial debond the value for G_a decreases. For a constant pressure rate the G_a approaches a value of 0.008 $lbf*in/in^2$, assuming a plate deformation. This is twice the value for a crystal specimen that had not been washed in water or acetone for the same pressurization rate. The specimen's mean value of G_a was still approximately the same as the unpolished crystals mean value. The solid horizontal line represents the mean value of adhesive fracture energy for this specimen using Andrews and Stevenson's equation to determine G_a. The unpolished specimen's plot is shown in Figure 15. The higher G_a found initially in the specimens was due to higher pressurization rates required to break the initial debond. These plots also show that G_a is a function of pressure rate. The higher the pressurization rate the higher the value of G_a for a given specimen.

Gent's values for G_a showed the tendency of being larger for the higher pressure rates. As the values for the pressure rate decreased so did G_a, but they did not quite level off and were still decreasing. As the pressure rate decreased the values computed for G_a for the plate and membrane approximations began to come closer to each other.

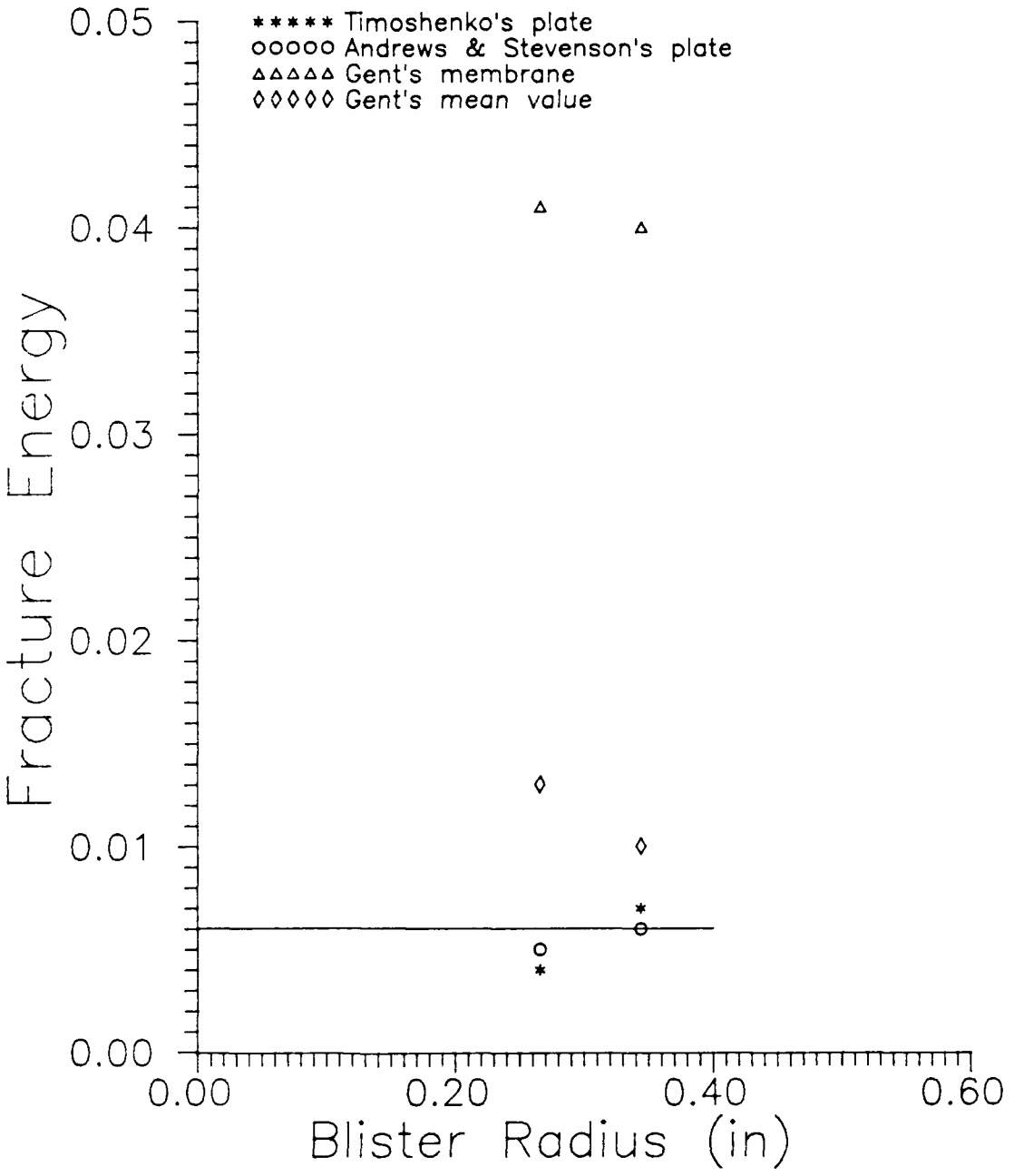

Figure 14. Adhesive Fracture Energy vs Blister Radius for Specimen # 12.

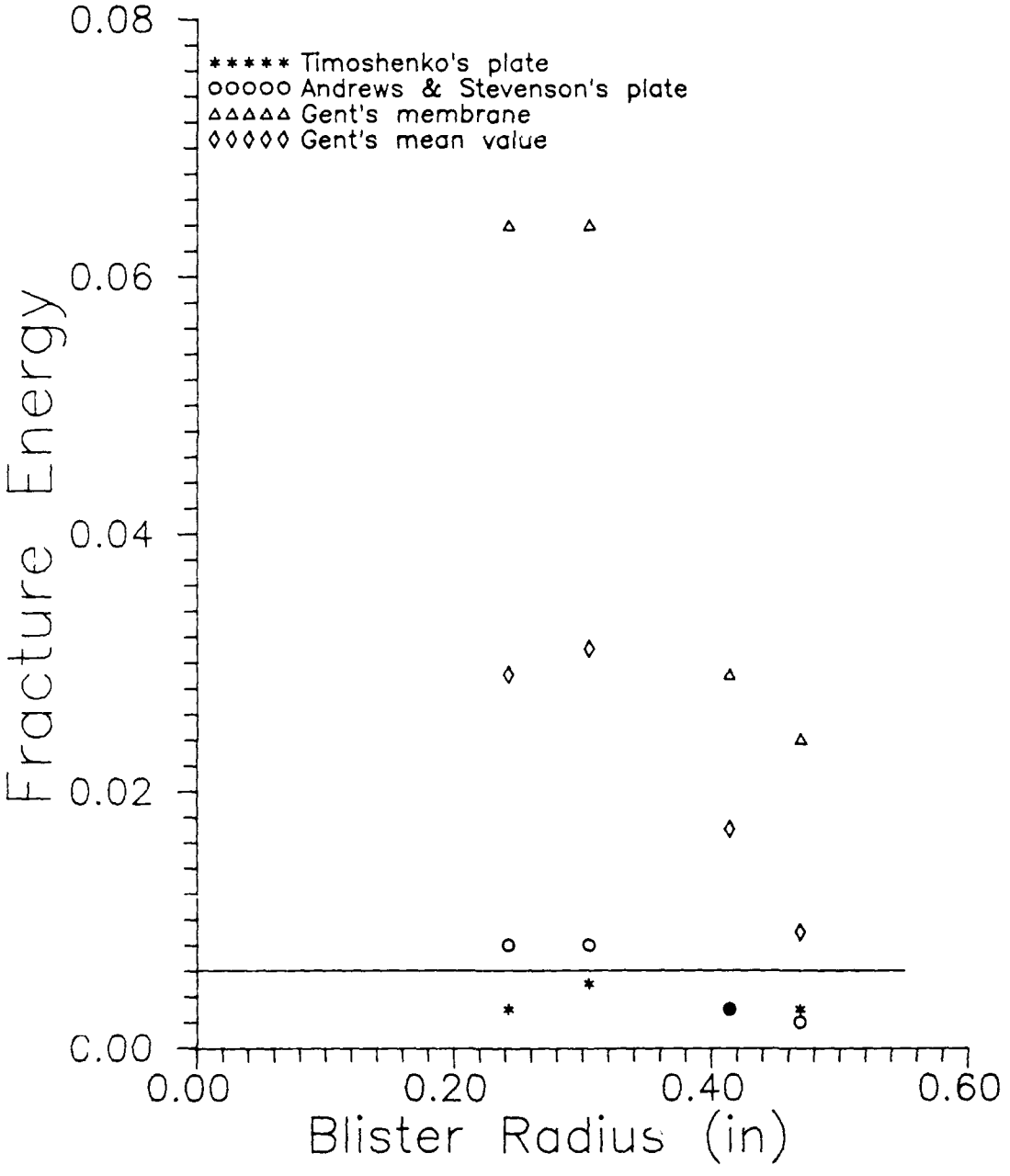

Figure 15. Adhesive Fracture Energy vs Blister Radius for Specimen # 9.

V. Conclusions and Recommendations

Conclusions

This experiment required the curing, initial debonding and computing of the adhesive fracture energy between an elastomeric layer and a crystalline substrate using a blister test. An appropriate method of curing the elastomeric material onto the crystal substrate and forming a uniform layer has been developed. The affects of humidity on the material have been limited. The adhesive is de-gassed prior to mixing and preheated in a vacuum oven. The vacuum maintains a constant pressure on the adhesive during the curing process so it will adhere to the crystal substrate.

An initial debond method has been developed. A thin film of silicone grease applied around the center of the specimen provides for an area where the adhesive will not bond to the substrate. A problem of air bubbles occasionally forming around the center region was encountered. This was caused by the water content present in the silicone grease. By limiting the amount of the silicone to just a small thin film these air pockets were reduced or eliminated.

The adhesive fracture energy can be calculated for a given pressure, elastic modulus, thickness, blister height and debond radius for this experiment. An LVDT measures the height of the blister. The blister behaves as a plate for thickness to radius ratios less than 0.5. Away from the

initial debond area the adhesive fracture energy is a constant $\pm$ 0.0015 lbf*in/in^2 for the same pressure rate in a specimen. Adhesive fracture energy was found to be a material property for certain test ratios of blister radius/deflection ratios for all three substrates tested. Andrews and Stevenson's method best computes G_a for the small deflections in the adhesive layer. Gent's values of G_a were better for the adhesive on the plexiglass substrate when it had large deflections and started to blow-up like a balloon with no adhesive fracture.

Recommendations

1. The following should be examined in further blister tests:
   a. Larger adhesive thickness to blister radius ratios be used to examine if the dimensionless plot of G_a becomes a constant. Increasing the adhesive thickness would be the easiest way to accomplish this.
   b. Increasing the pressurization rates to between 10 and 10^6 psi/sec to examine if G_a similar to that found by Andrews and Stevenson is obtained.
   c. Examine if the G_a is a function of pressurization rate. An air flow meter could be used for this.
   d. Examine the affect of different surface preparations on G_a, such as. sanding, washing or

polishing of the substrate surface.

e. If higher pressurization rates are used a method of visually recording the blister growth without raising the temperature of the specimen must be found. Possible methods would include: holography or a high speed camera using a very high pressurization rate to minimize the heat affect of the lights.

f. Larger blister radius/deflection ratios be used to examine if G_a is a material property for all these ratios.

2. The test be continued with the following modifications to the test equipment:

a. An epoxy with material properties better approximating the solid rocket fuel be used, such as R-45M and MDI.

b. The specimens should be prepared by a chemist so the exact stoichiometry is maintained in each specimen. This is because a chemist is required to produce consistent adhesive layers in the amount of time and equipment available.

c. The output voltages from the pressure transducer and LVDT should be sent directly to a computer via an analog to digital converter so the test may be run without any interruptions.

d. An air flow meter be used to more accurately

control the pressurization rate.

e. An adhesive teflon tape be used in place of silicone grease in the mold and in the region of initial debond. This should reduce all the sources of moisture in the adhesive and eliminate the air bubbles.

Bibliography

1. Andrews, E. H. and A. Stevenson, "Fracture Energy of Epoxy Resin Under Plane Strain Conditions," Journal of Materials Science. Vol 13: 1680-1688 (Aug 1978).

2. Bascom, W. D. and R. L. Cottington, "Effect of Temperature on the Adhesive Fracture Behavior of an Elastomer-Epoxy Resin," Journal of Adhesion. Vol 7: 333-346 (1976).

3. Bennett, S. J., K. L. Devries and M. L. Williams, "Adhesive Fracture Mechanics," Journal of Fracture. Vol 10: 33-43 (March 1974).

4. Broutman, L. J. and F. J. McGarry, "Fracture Surface Work Meeasurements on Glassy Polymers by a Cleavage Technique," Journal of Applied Polymer Science. Vol 9: 589-608 (1965).

5. Dannenberg, Hans, "Measurement of Adhesion by a Blister Method," Journal of Applied Polymer Science. Vol V, Issue No 14: 125-134 (1961).

6. Gent, A. N. and L. H. Lewandowski, "Blow-Off Pressures for Adhering Layers," Office of Naval Research Technical Report No. 7. Project NR 092-555, November 1986.

7. Gent, A. N., "New and Improved Tests for Adhesion," Office of Naval Research Technical Report No. 9. Project NR 092-555, May 1987.

8. Hinkley, J. A., "A Blister Test for Adhesion of Polymer Films to SiO2," Journal of Adhesion. Vol 16: 115-126 (Nov 1983).

9. Jones, P. F., "Report No 30988, Dogbone/Stress Relaxation," Laboratory Report Analytical Chemical Services NTS Engineering. AFAL/MKPB, Edwards AFB, CA, (Sept 1988).

10. Jones, W. B., "Blister Tests for Adhesive Fracture," National Sampe Technical Conference Proceedings. Vol 2: 145-148, (1970)

11. LVDT Product Catalog, Robinson-Halpern Co., Plymouth Meeting, PA (19462).

12. Mai, Y. W. and A. G. Atkins, "Letter to Selby and Miller," Journal of Material Science. Vol 10: 2000 (1975).

13. Philip, John, Construction Sealants and Adhesives. New York: John Wiley & Sons, Inc, (1970).

14. Schreuder-Stacer, H., AFAL/MKPB. Telephone Interview. Edwards AFB, CA, 30 Aug 88.

15. Schreuder-Stacer, H., AFAL/MKPB. Personal Interview. Wright-Patterson AFB, 21 Oct 88.

16. Selby, K. and L. E. Miller, "Fracture Toughness and Mechanical Behavior of an Epoxy Resin," Journal of Material Science. Vol 10: 12-24 (1975).

17. Skeist, Irving (editor), Handbook of Adhesives. New York: Von Nostrand Reinhold Co., (1977).

18. Sneddon, Ian N. and Morton Lowengrub, Crack Problems in the Classical Theory of Elasticity. New York: John Wiley & Sons, Inc, 1969.

19. Timoshenko, Stephen and J. N. Goodier, Theory of Elasticity. New York: McGraw-Hill Book Company, Inc, 1951.

20. Timoshenko, Stephen and S. Woinowsky-Krieger, Theory of Plates and Shells. New York: McGraw-Hill Book Publishing Co, 1959.

21. Williams, M. L., "The Continuum Interpretation for Fracture and Adhesion," Journal of Applied Polymer Science. Vol 13: 29-40 (1969).

Appendix A. Equipment List

Equipment List

Silicone lubricant. High vacuum grease

Lubricating silicone compound

Disk specimens plexiglass and sodium chloride
Dimensions: 2, 3" diameter and 3" square.

Scales: Balance triple beam accuracy $\pm$ 0.02 gm

Molds. 2", 3" diameter and 3" square, fabricated of aluminum and 3" in depth

Graduated cylinder

Glass dishes 3" diameter and concave

Spatula

Level

Teflon tape

Metal pin sized to fit the air inlet hole of the specimen

Traveling microscope accuracy $\pm$ 0.001"

Vacuum oven Capable of maintaining $65^{\circ} \pm 5^{\circ}$ and a vacuum of -25 to -29" HG. Inner size: at least 9x9x9"

LVDT range $\pm$ 0.30"

Pressure transducer capable of at least 5.35 mV/psi

LVDT calibrator accuracy: $\pm$ 0.001"

Function generator

Voltmeter

Barton pressure calibrator

Power supply AC and DC to 10 Volts

Low pressure air, 60 psi $\pm$ 0.04 psi

Storage oscilloscope and computer program (GURU)

Appendix B: Test Procedures

Curing Procedures

1. Always use rubber gloves when handling specimens so moisture is not absorbed by the specimen.

2. Weigh the substrate on a balance triple beam scale.

3. Fill the hole in the center of the substrate with a metal pin coated in teflon tape, and mount it flush with the top surface of the substrate. The pin should stick out of the bottom of the substrate enough so it may be removed, about 0.25".

4. Place the mold in the vacuum oven and level the mold with a bubble level by adjusting the legs of the mold.

5. Remove the mold from the oven and coat the inside and top surface with silicone grease.

6. Coat the substrate's sides and bottom sparingly with silicone grease and place the substrate in the mold.

7. Place a circular template, 7/16" diameter, on the center of the substrate and put a slight trace of silicone grease in the template.

8. Weigh the epoxy, R-45 and HT, separately and put them on glass dishes. Ratio is 10 grams R-45 with 0.26 grams HT.

9. Place dish with the R-45 in the vacuum oven and de-gas and heat the oven to 50° C and at least -25 " HG to warm up the epoxy. Maintain this temperature for at least 30 minutes.

10. Vent oven and remove the dish.

11. Add isocyanate to the epoxy and mix by hand.

12. Place the dish back in the oven and evacuate it for 2 minutes at 50° C and -25" HG.

13. Vent the oven and remove the dish.

14. Mix the adhesive.

15. Place the dish back in the oven and evacuate it for 5 minutes at 50° C and -25" HG.

16. Vent the oven and remove the dish.

17. Mix the adhesive.

18. Place the dish back in the oven and evacuate it for 5 minutes at 50° C and -25" HG.

19. Vent the oven and remove the dish.

20. Pour the adhesive onto the substrate and spread it evenly over the substrate with the spatula.

21. Place the mold in the oven and evacuate it for 24 hours at $65^{\circ} \pm 5^{\circ}$ C and -25" HG to cure.

22. After 24 hours turn the oven off and vent it.

23. Remove the mold from the oven after it cools to room temperature, approximately 8 hours.

24. Remove the specimen from the mold with a metal rod pushed through the bottom of the mold.

Blister Test Procedures

1. Measure the thickness of the adhesive on the substrate with a traveling microscope. Taking at least 16 evenly spaced measurements and use the average value in computing G_a.

2. Set up the equipment as in Figure 6. Turn on the equipment and warm it up.

3. Place the specimen in the holder, insert air line, and center the LVDT over the specimen. Ensure the LVDT voltage is in the calibrated linear range (2.35 V to 5.65 V).

4. Mark the initial radius of the blister on the specimen as the template radius used in the curing process with a pen.

5. On the oscilloscope set 5 secs/div, channel 1 as the output from the pressure transducer, and channel 2 as the output from the LVDT.

6. Manually trigger the oscilloscope and slowly open the air regulator, watching the voltages of the pressure transducer and LVDT to ensure data is being taken.

7. When the radius of the blister exceeds the initial radius reduce the pressure on the specimen to keep debond from occurring.

8. At the end of the test period, 102.3 seconds, transfer the data from the oscilloscope to the computer disk.

9. Continue with steps 6 through 8 until debond of the adhesive from the substrate occurs. Mark the new blister radius on the specimen before beginning the test again with the pen.

10. After debond transfer the stored data from voltage to pressure and height using time as the synchronizing mode.

11. Compute fracture energy.

Appendix C: Experimental Test Data

Table 7. Specimen Geometry and Material

Specimen #	Substrate	
	Material	Size (in±.01")
1	plexiglass	3.00 square
2	plexiglass	2.00 diameter
3	plexiglass	2.00 diameter
4	plexiglass	3.00 square
5	plexiglass	2.00 diameter
6	crystal	1.94 diameter
7	crystal	1.94 diameter
8	crystal	1.94 diameter
9	crystal	3.00 diameter
10	crystal	1.94 diameter
11	crystal	3.00 diameter
12	crystal	1.94 diameter

Table 8. Experiment Output Data *

Specimen #	Adhesive Thickness ±.001"	P_{cr} (psi) ±.04	Height (inches) ±.001"	Radius (inches) ±.1/128"
1	0.0738	15.00	0.13242	0.3125
2	0.0743	21.80	0.069789	0.328125
		20.72	0.103789	0.40625
		16.20	0.157472	0.50000
		14.48	0.211156	0.515625
		13.20	0.336419	0.609375
3	0.0735	6.81	0.013420	0.234375
		11.96	0.139580	0.28125
		3.995	0.135990	0.46875
		4.33	0.19326	0.54687
4	0.0712	16.84	0.11989	0.234375
		15.60	0.13242	0.265625
		15.49	0.36505	0.40625
5	0.0595	8.7	0.1790	0.234375
		7.67	0.17689	0.390625
		7.80	0.21040	0.4375
		7.17	0.20110	0.453125
		8.40	0.41989	0.46875
6	0.010	2.09	0.092441	0.390625
		2.30	0.096019	0.46875
		1.82	0.19251	0.546875
7	0.0967	7.75	0.03436	0.1875
8	0.090	5.26	0.01074	0.1875
		4.55	0.01360	0.304688
		1.82	0.01145	0.34375
		1.39	0.01432	0.382813
9	0.1366	3.37	0.01816	0.15625
		2.31	0.01906	0.242188
		1.83	0.02648	0.304688
		0.75	0.03507	0.414063
		0.56	0.02443	0.46875

continued on the next page.

Specimen #	Adhesive Thickness	p_{cr} (psi)	Height (inches)	Radius (inches)
10	0.09485	1.692	0.05869	0.3750
		2.068	0.67105	0.5625
11	0.0796	1.993	0.001789	0.21094
		0.961	0.013599	0.39844
		0.99076	0.010210	0.55469
12	0.0995	2.4816	0.005727	0.21875
		1.37616	0.014316	0.26563
		1.04904	0.015031	0.34375

* The initial values for each test specimen were not used in computing an average value of G_a.

Appendix D: Blister Test Data

Figures 16 through 24. Range of G_a for Specimens 2 through 12.

Figures 25 through 33. Blister Pressure versus Height until Adhesive Fracture for Specimens 1 through 12. Theoretical values for a clamped Timoshenko plate and an Andrews and Stevenson plate are shown by the solid and dashed lines above the plotted data points. A solid line below the data is for a simply supported Timoshenko plate boundary condition. Figures 27, 28, 31, 32 and 33 show change in pressure versus change in height.

Figures 34 to 35. Adhesive Fracture Energy versus a/t Ratio for Plexiglass and Unpolished Crystal Substrates.

Figures 36 to 37. Adhesive Fracture Energy versus h/t Ratio for Plexiglass and Unpolished Crystal Substrates.

The figures below show the average values from Tables 2, 3 and 4 and the range over which G_a varied for each specimen.

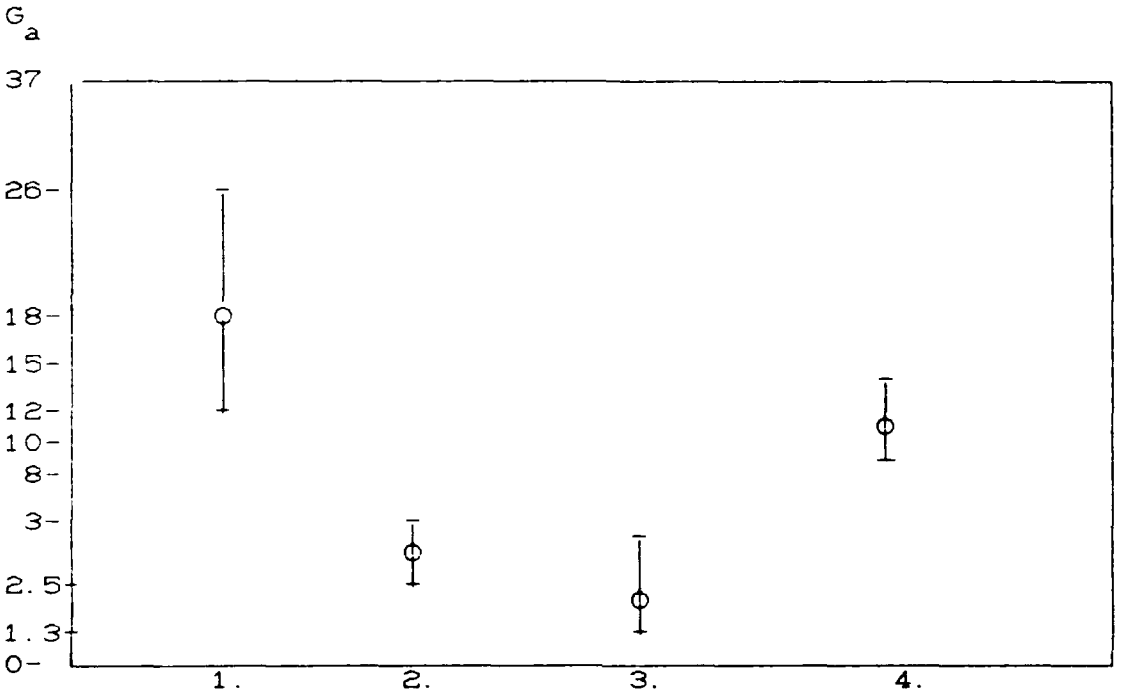

Figure 17. Range of G_a for Specimen 2

1. Timoshenko's Plate Theory, Equation 15
2. Gent's Membrane Theory, Equation 23
3. Gent's mean value, Equation 22
4. Andrews and Stevenson's Plate, Equation 21

Plot is based on 4 data points for each mathematical model.

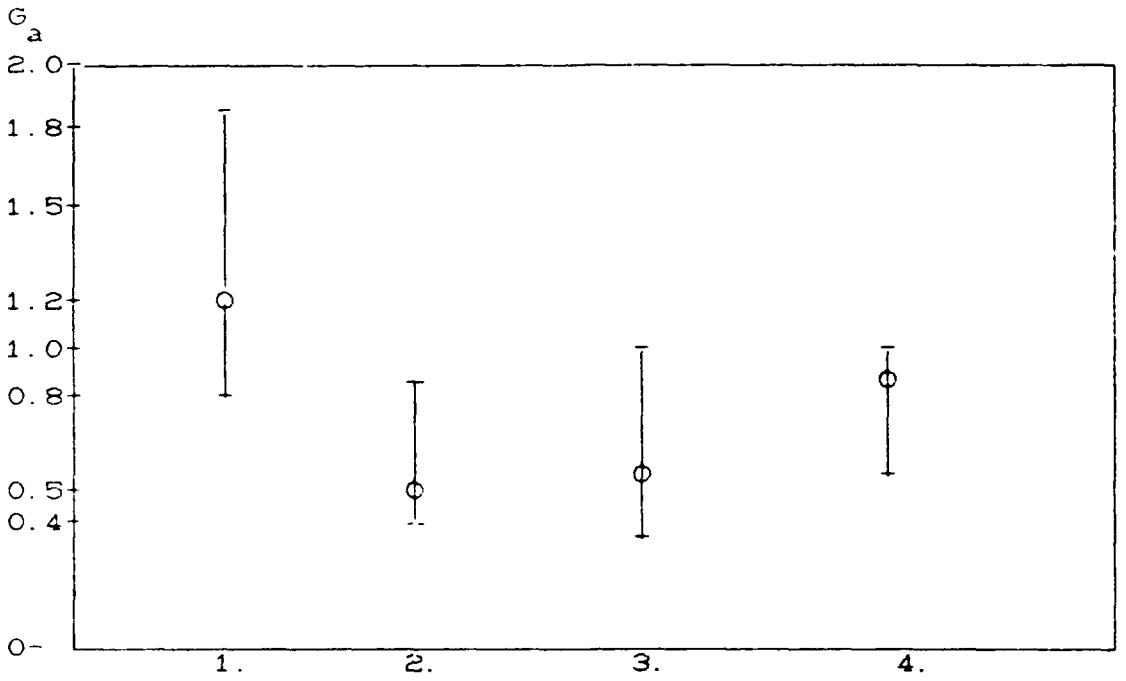

Figure 18. Range of G_a for Specimen 3

1. Timoshenko's Plate Theory, Equation 15
2. Gent's Membrane Theory, Equation 23
3. Gent's mean value, Equation 22
4. Andrews and Stevenson's Plate, Equation 21

Plot is based on 3 data points for each mathematical model.

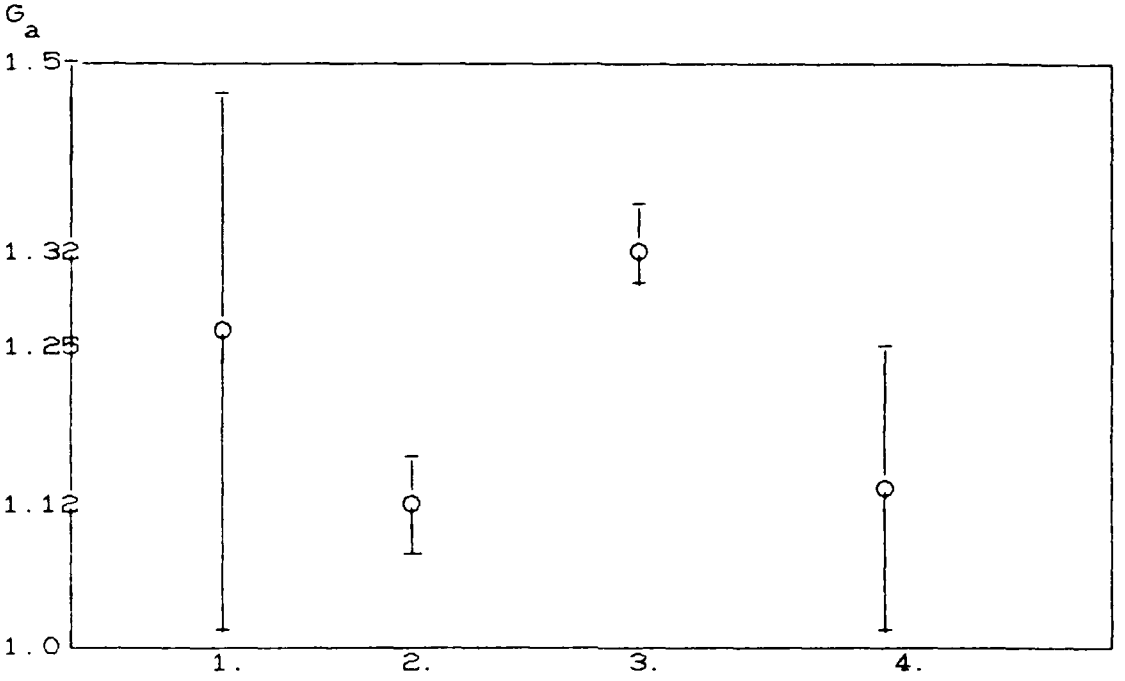

Figure 19. Range of G_a for Specimen 4

1. Timoshenko's Plate Theory, Equation 15
2. Gent's Membrane Theory, Equation 23
3. Gent's mean value, Equation 22
4. Andrews and Stevenson's Plate, Equation 21

Plot is based on 2 data points for each mathematical model.

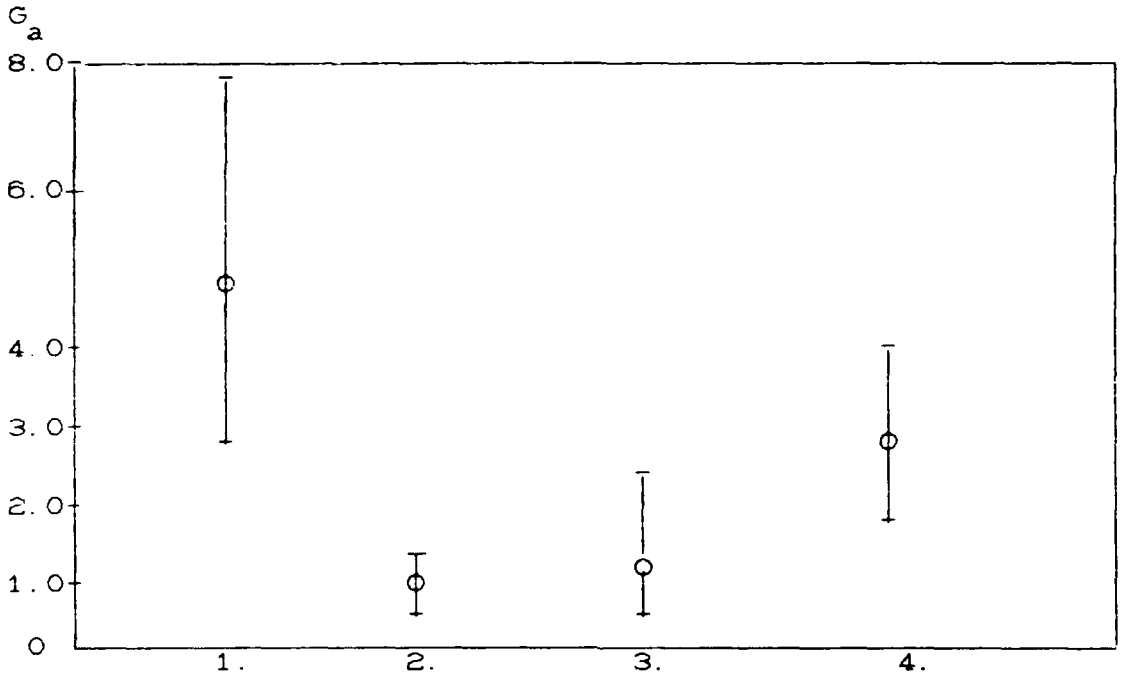

Figure 20. Range of G_a for Specimen 5

1. Timoshenko's Plate Theory, Equation 15
2. Gent's Membrane Theory, Equation 23
3. Gent's mean value, Equation 22
4. Andrews and Stevenson's Plate, Equation 21

Plot is based on 4 data points for each mathematical model.

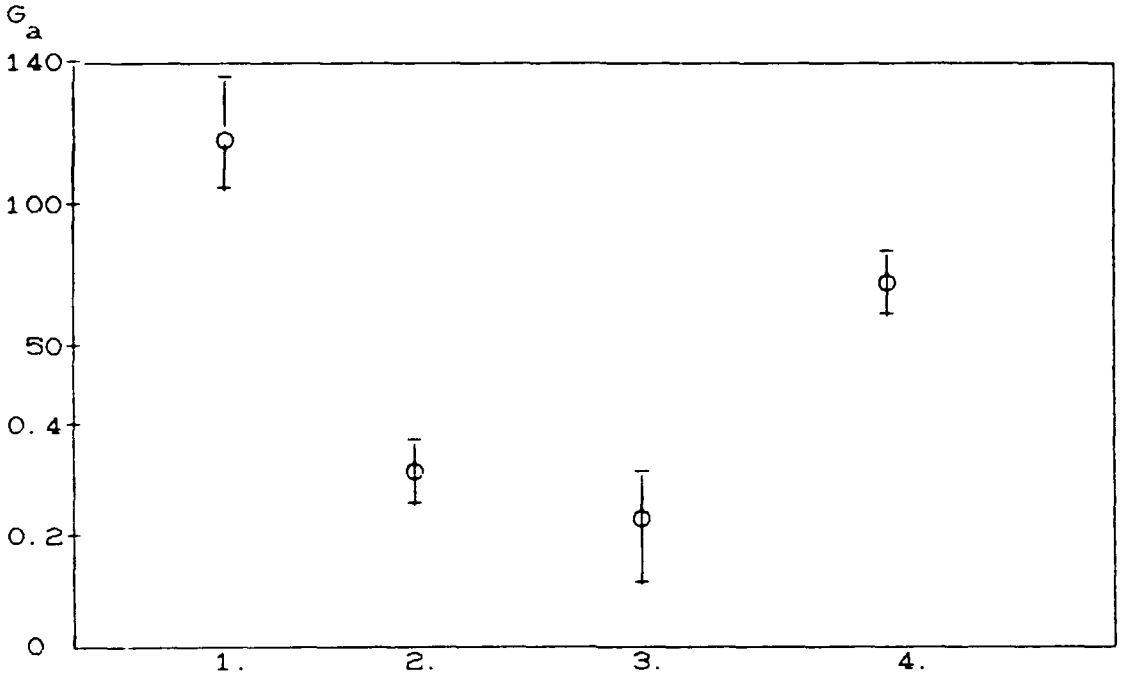

Figure 21. Range of G_a for Specimen 6

1. Timoshenko's Plate Theory, Equation 15
2. Gent's Membrane Theory, Equation 23
3. Gent's mean value, Equation 22
4. Andrews and Stevenson's Plate, Equation 21

Plot is based on 2 data points for each mathematical model.

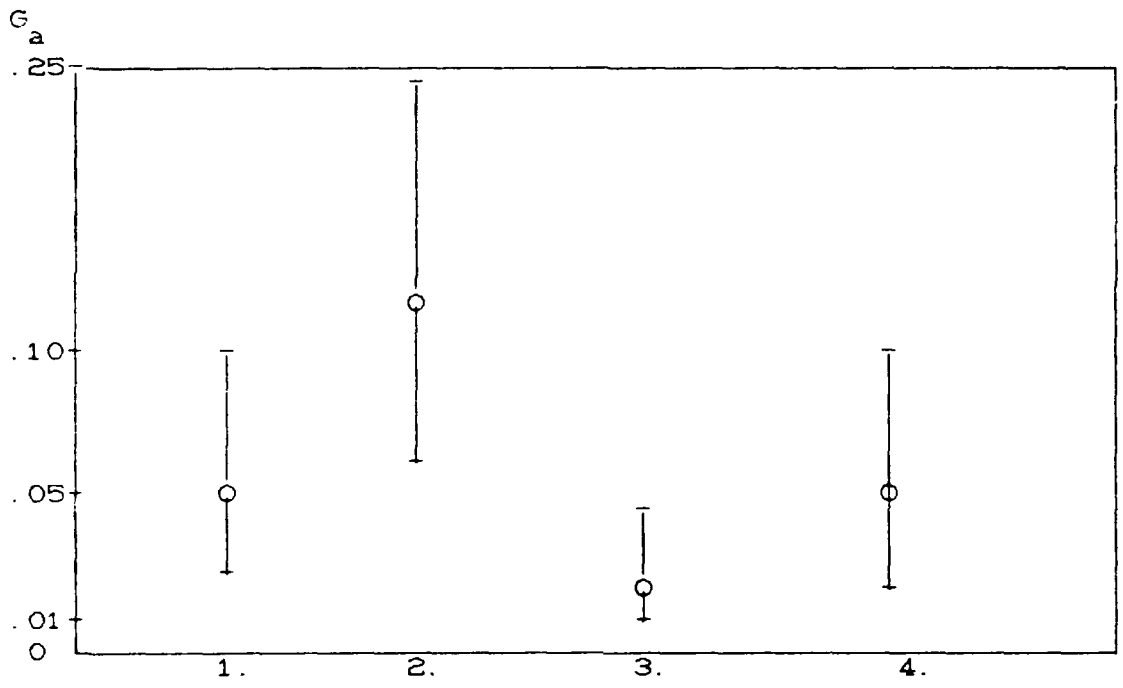

Figure 22. Range of G_a for Specimen 8

1. Timoshenko's Plate Theory, Equation 15
2. Gent's Membrane Theory, Equation 23
3. Gent's mean value, Equation 22
4. Andrews and Stevenson's Plate, Equation 21

Plot is based on 3 data points for each mathematical model.

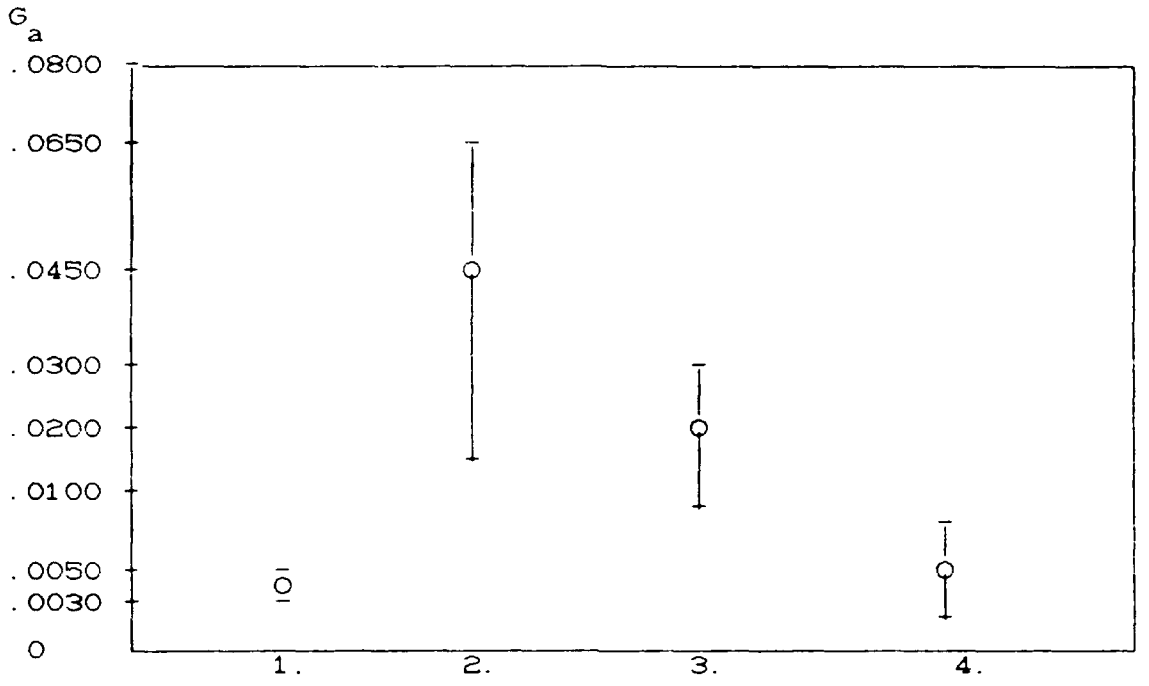

Figure 23. Range of G_a for Specimen 9

1. Timoshenko's Plate Theory, Equation 15
2. Gent's Membrane Theory, Equation 23
3. Gent's mean value, Equation 22
4. Andrews and Stevenson's Plate, Equation 21

Plot is based on 4 data points for each mathematical model.

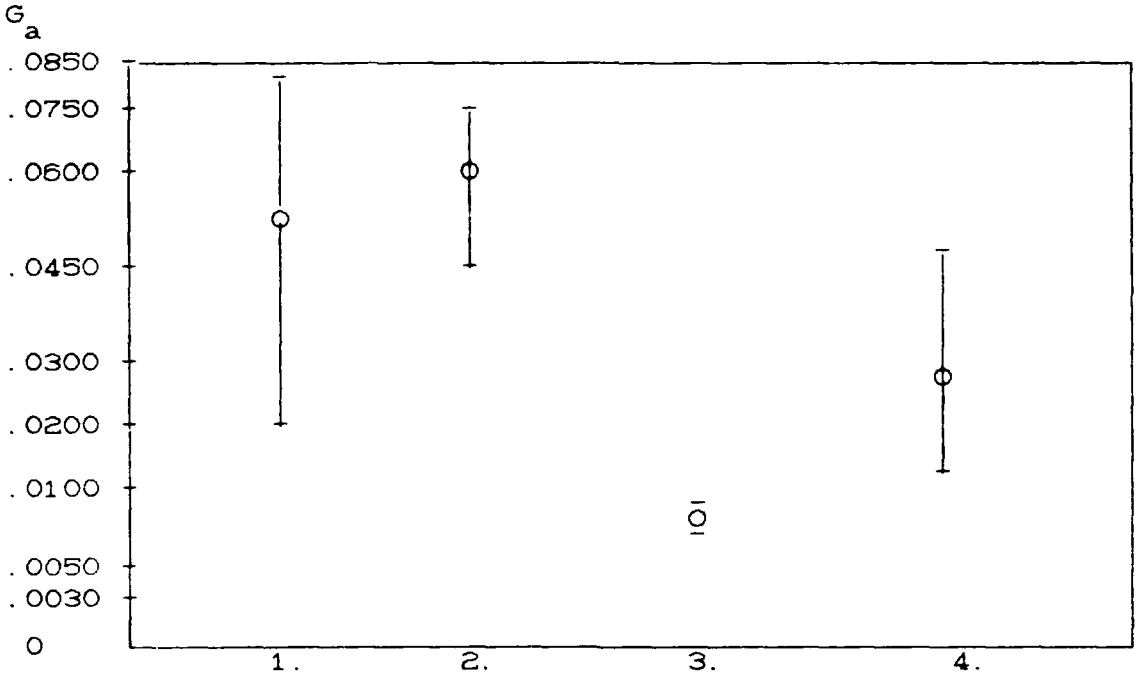

Figure 24. Range of G_a for Specimen 11

1. Timoshenko's Plate Theory, Equation 15
2. Gent's Membrane Theory, Equation 23
3. Gent's mean value, Equation 22
4. Andrews and Stevenson's Plate, Equation 21

Plot is based on 2 data points for each mathematical model.

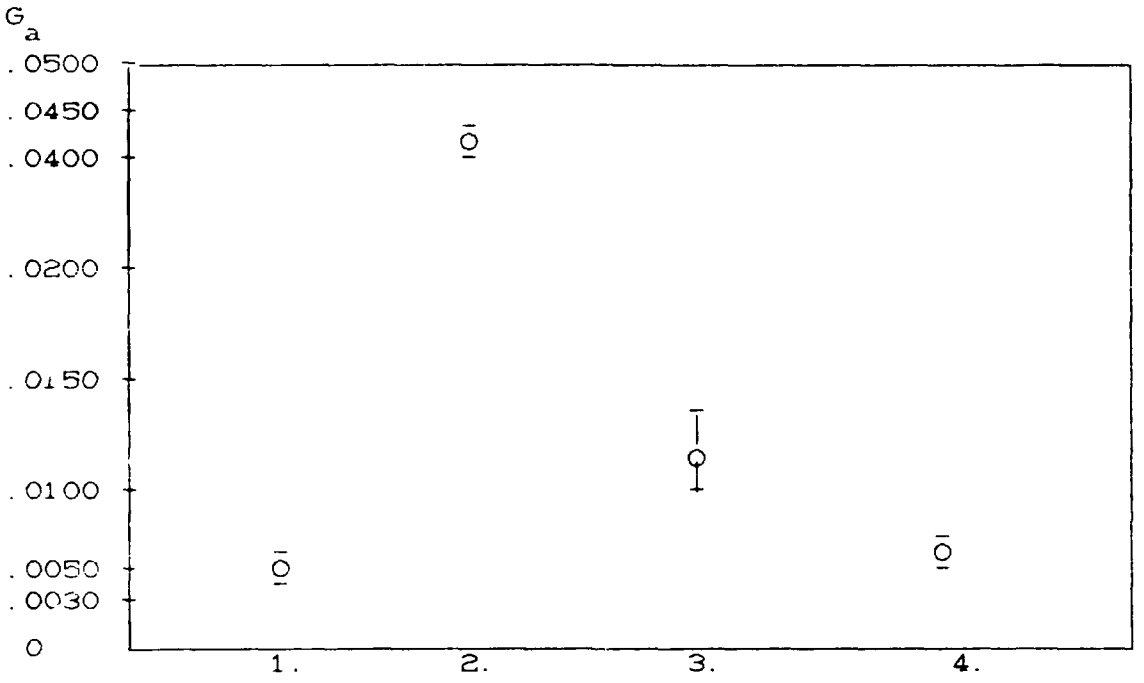

Figure 25. Range of G_a for Specimen 12

1. Timoshenko's Plate Theory, Equation 15
2. Gent's Membrane Theory, Equation 23
3. Gent's mean value, Equation 22
4. Andrews and Stevenson's Plate, Equation 21

Plot is based on 2 data points for each mathematical model.

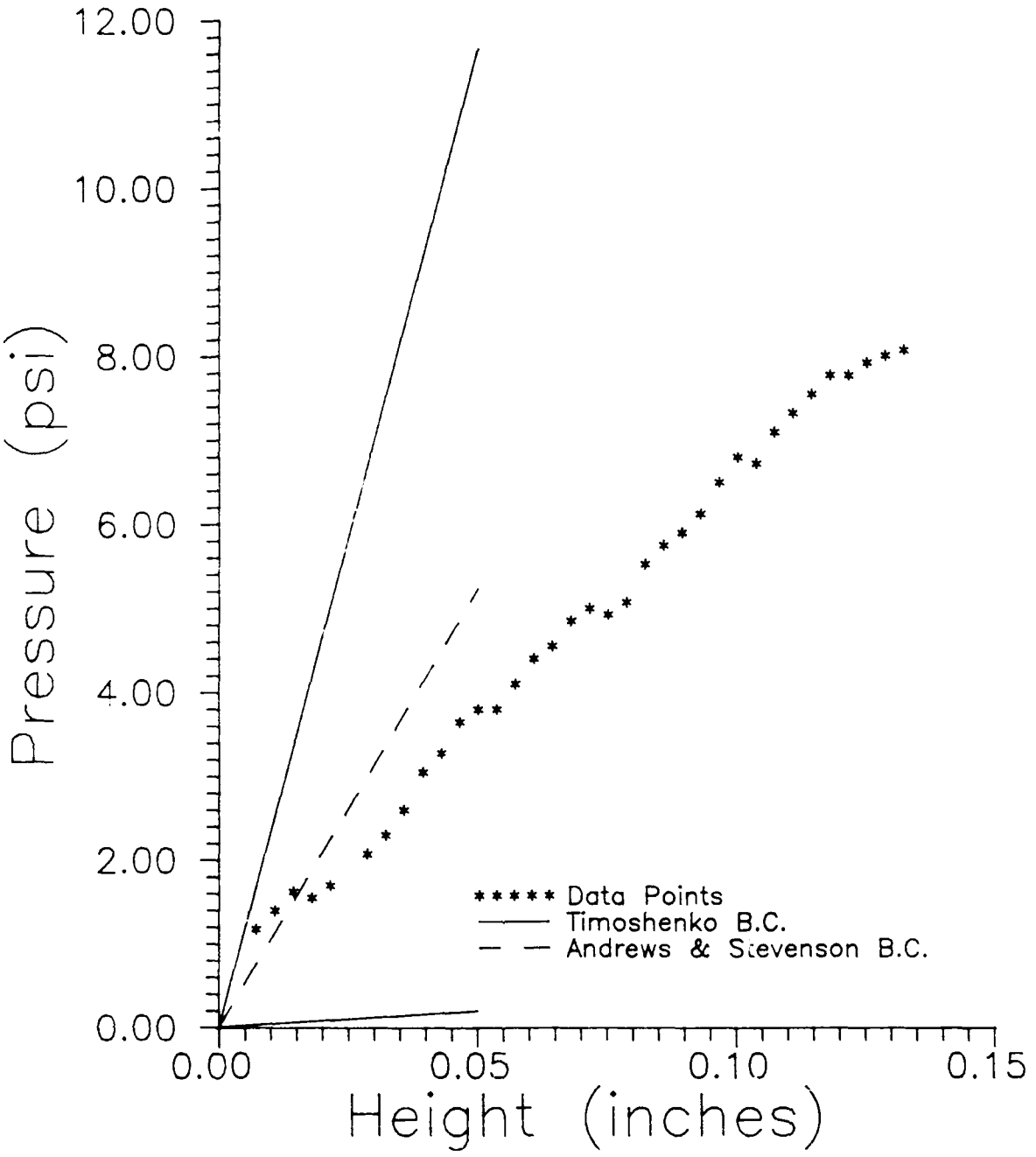

Figure 25. Blister Pressure versus Height until Adhesive Fracture Specimen No. 1. Test Date 21 Sep 88.

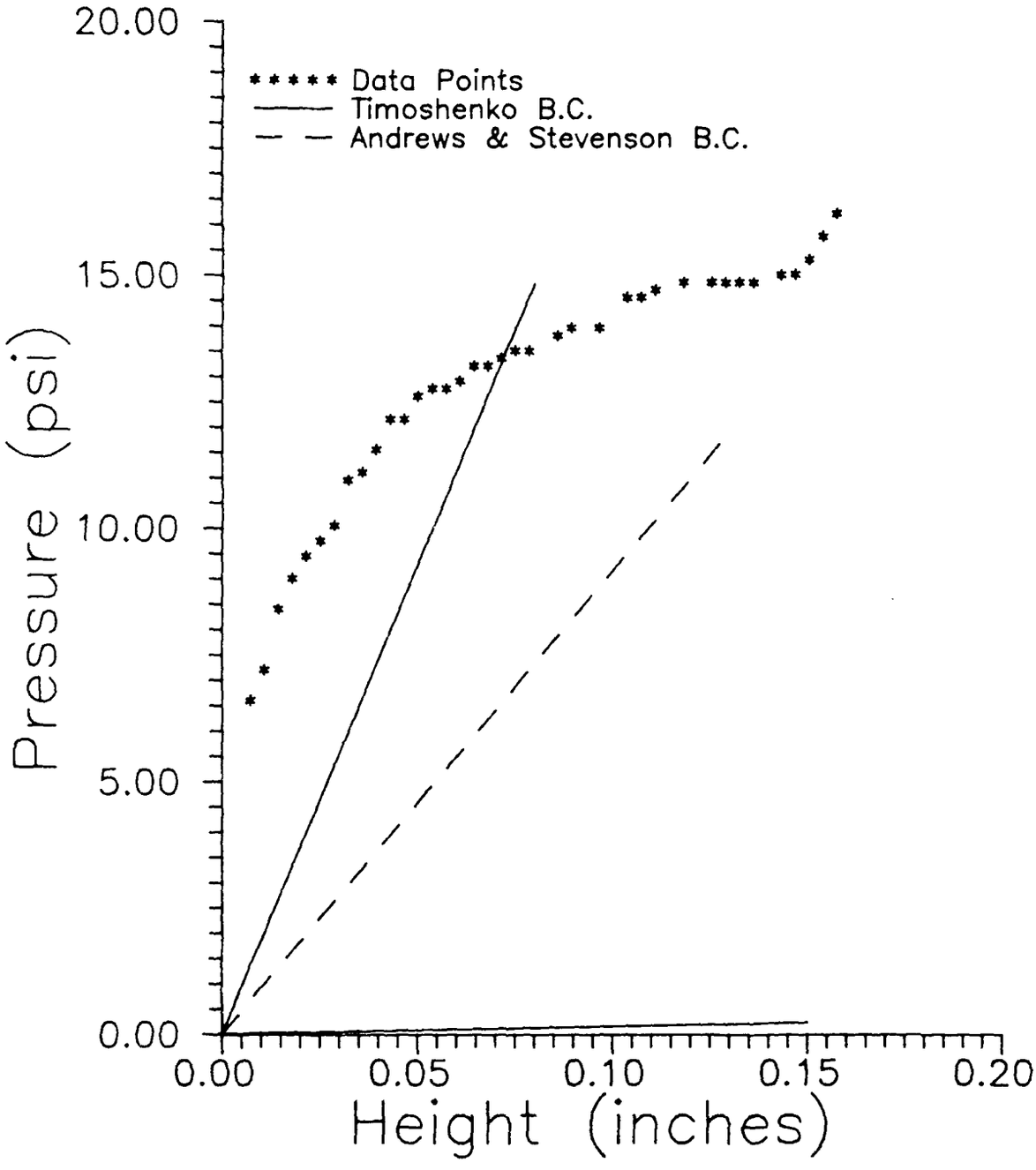

Figure 26. Blister Pressure versus Height until Adhesive Fracture Specimen No. 2. Test Date 23 Sep 88.

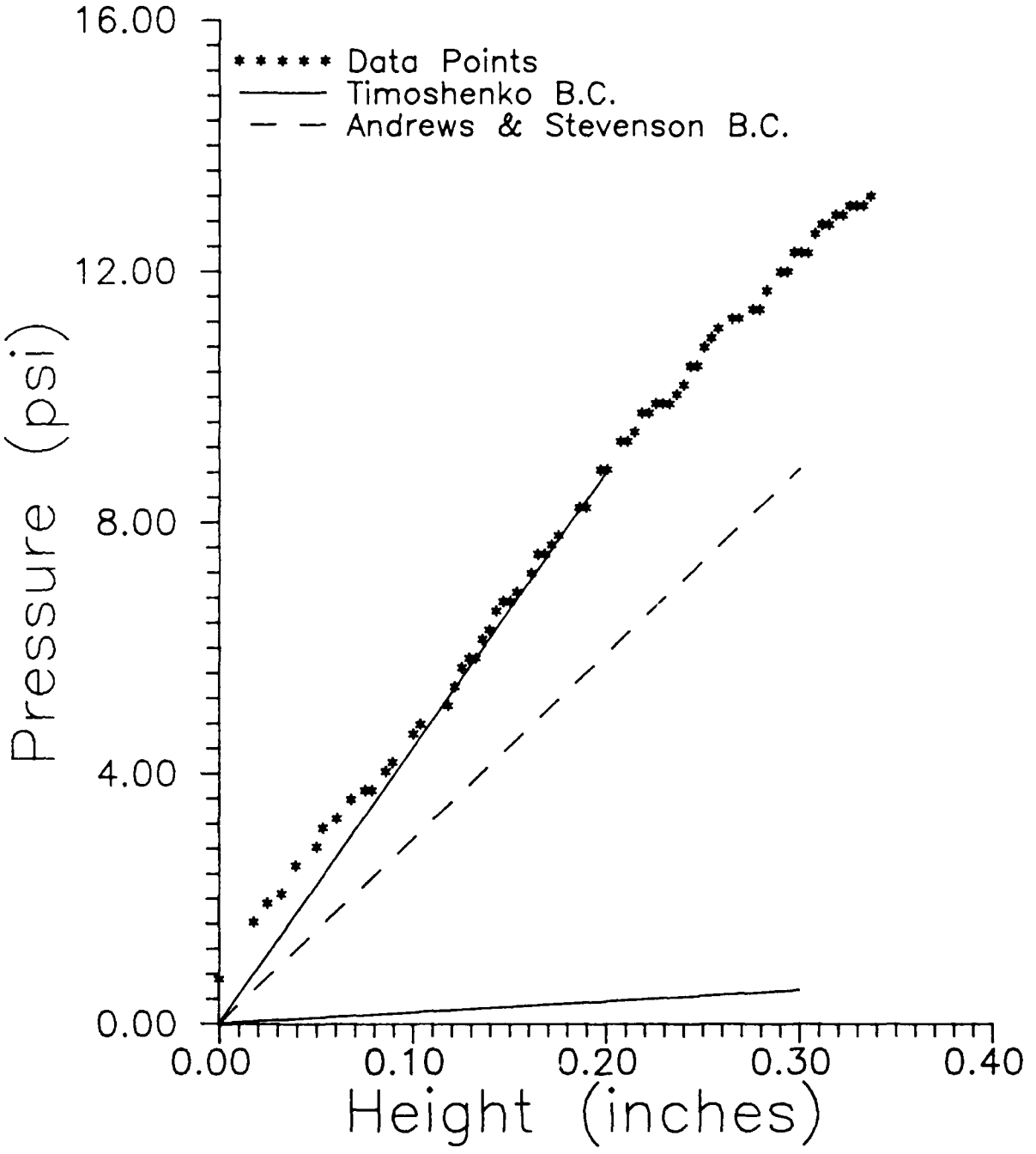

Figure 27. Blister Pressure versus Height until Adhesive Fracture Specimen No. 2. Test Date 23 Sep 88.

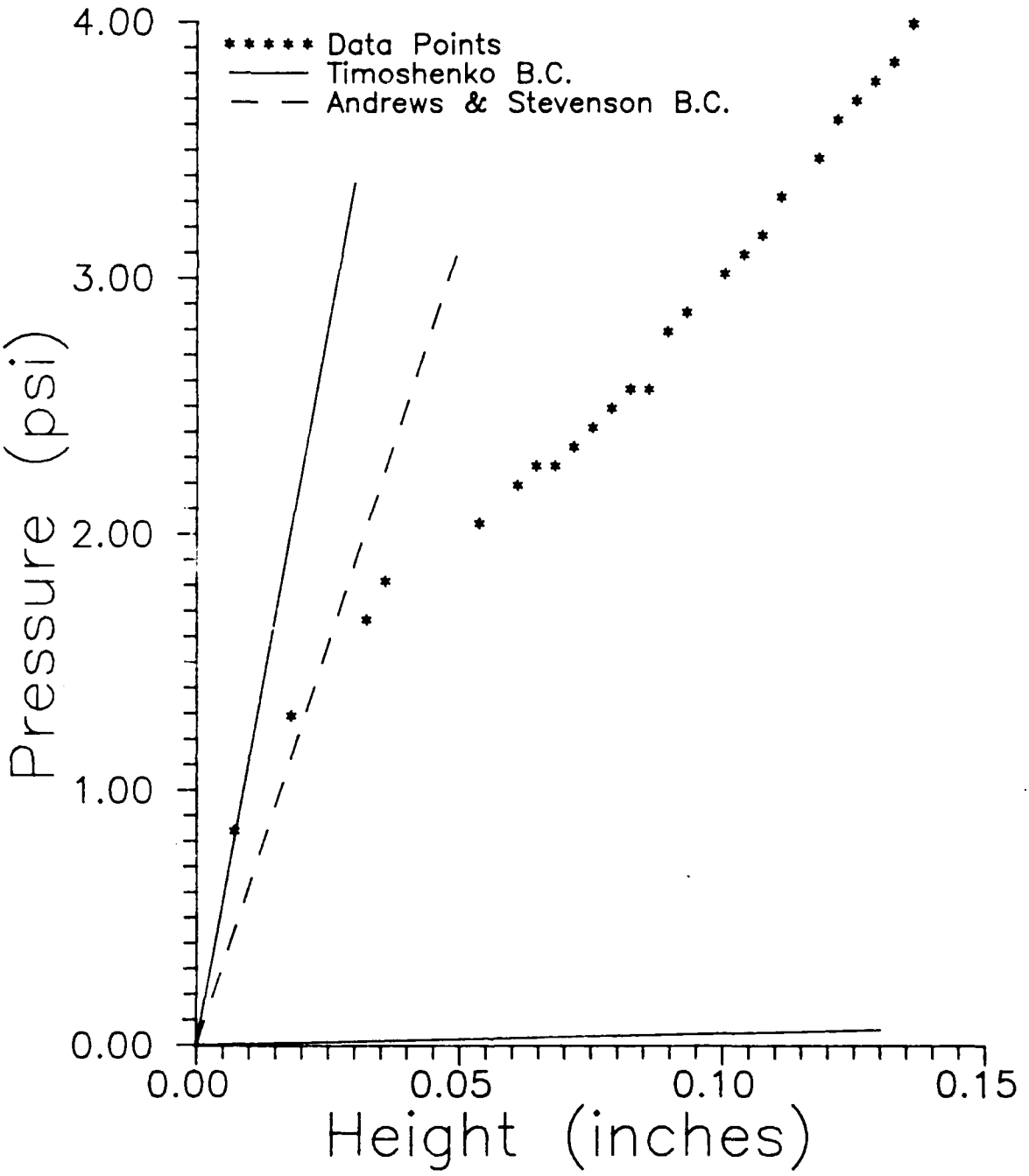

Figure 28. Blister Pressure versus Height until Adhesive Fracture Specimen No. 3. Test Date 28 Sep 88.

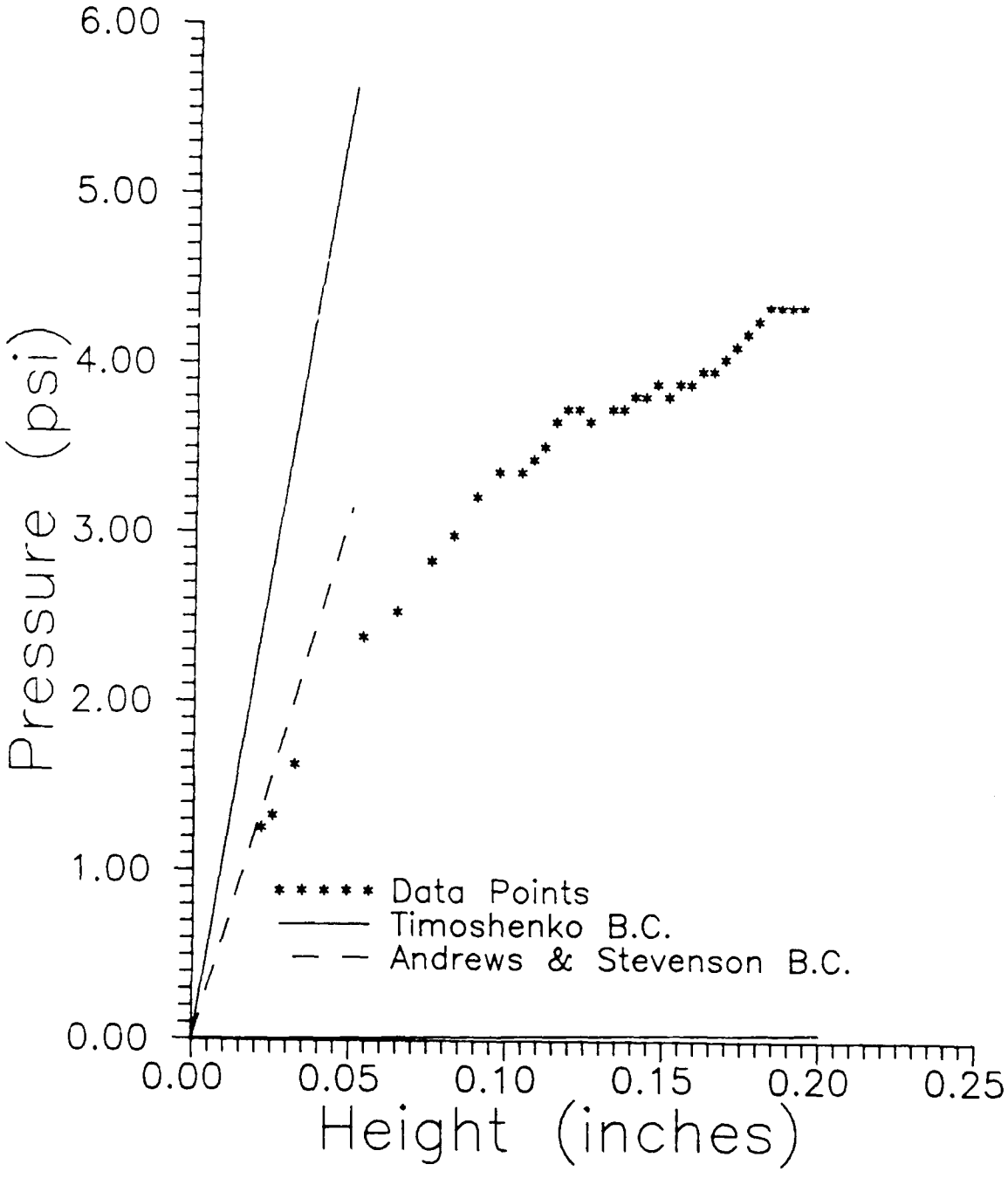

Figure 29. Blister Pressure versus Height until Adhesive Fracture Specimen No. 3. Test Date 28 Sep 88.

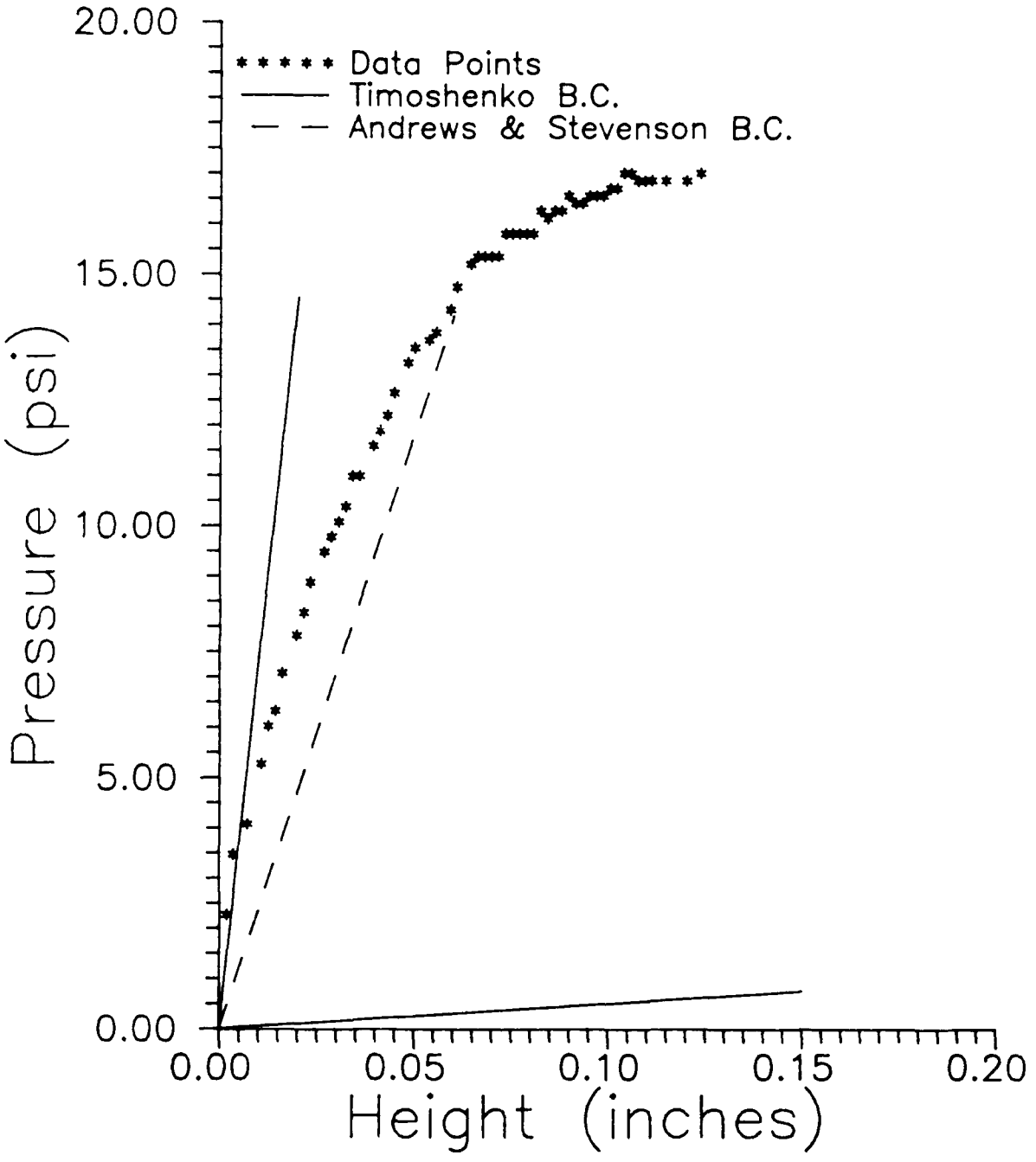

Figure 30. Blister Pressure versus Height until Adhesive Fracture Specimen No. 4. Test Date 28 Sep 88.

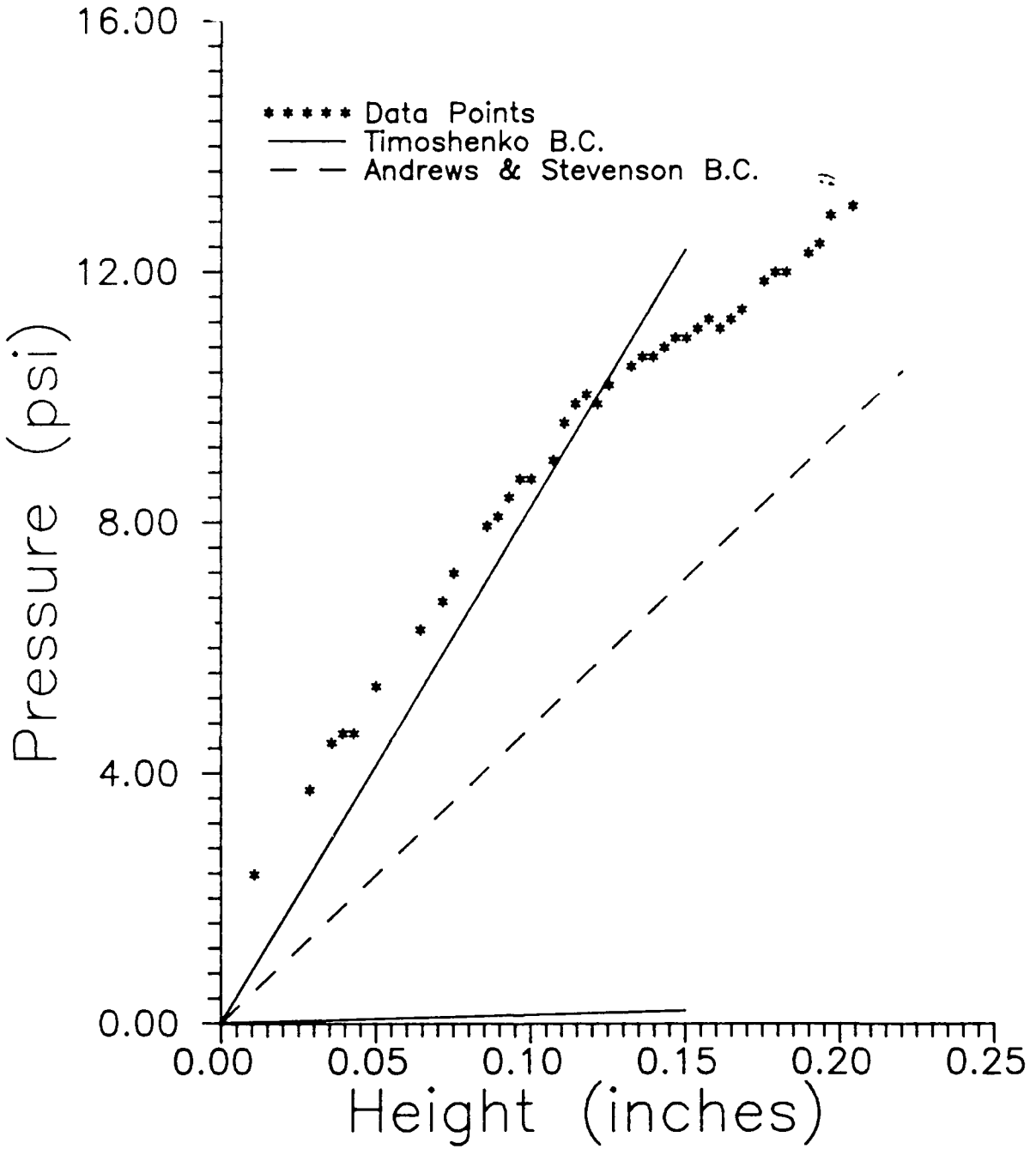

Figure 31. Blister Pressure versus Height until Adhesive Fracture
Specimen No. 4. Test Date 28 Sep 88.

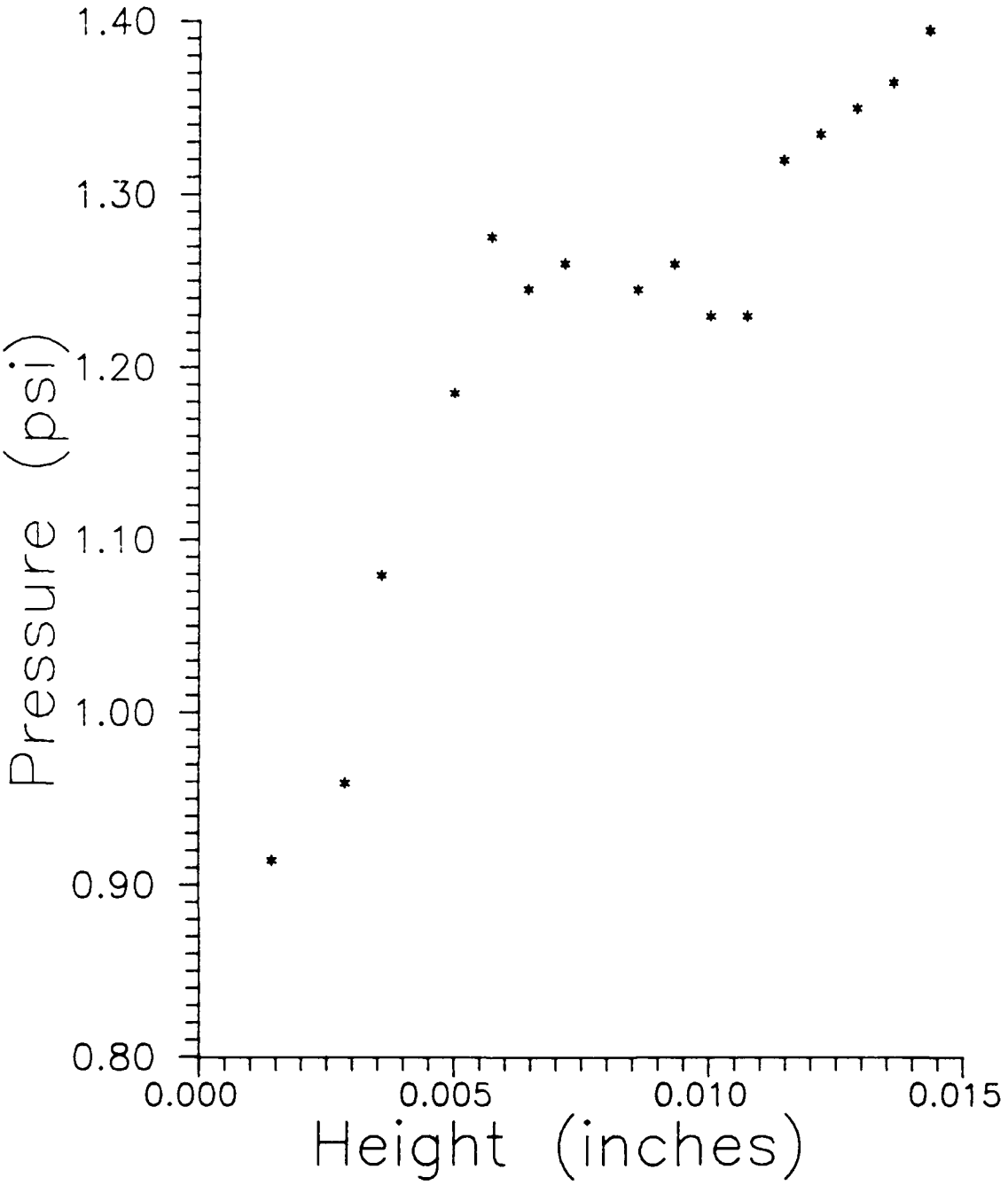

Figure 32. Blister Pressure versus Height until Adhesive Fracture Specimen No. 8. Test Date 16 Oct 88.

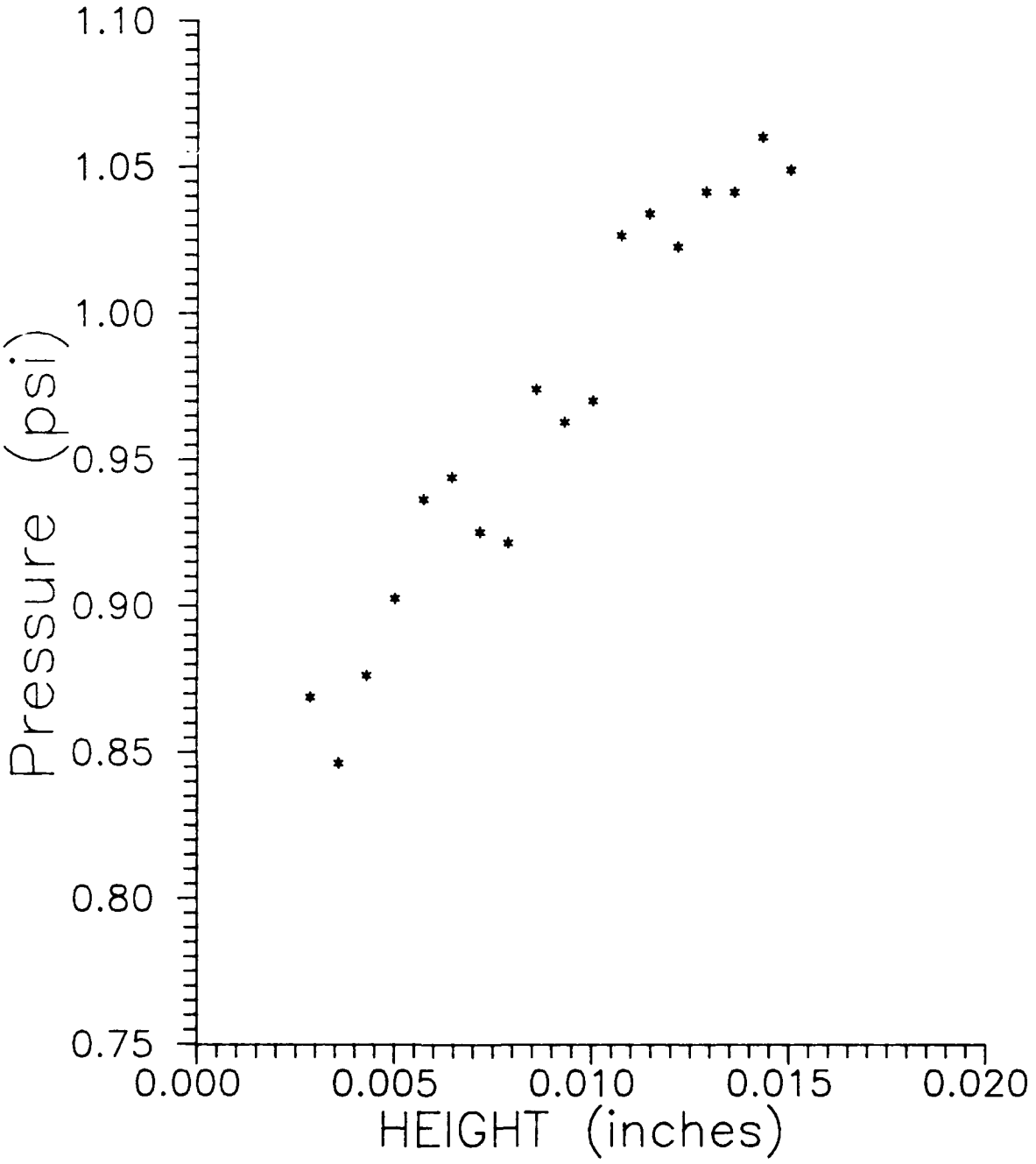

Figure 33. Blister Pressure versus Height until Adhesive Fracture Specimen No. 12. Test Date 26 Oct 88.

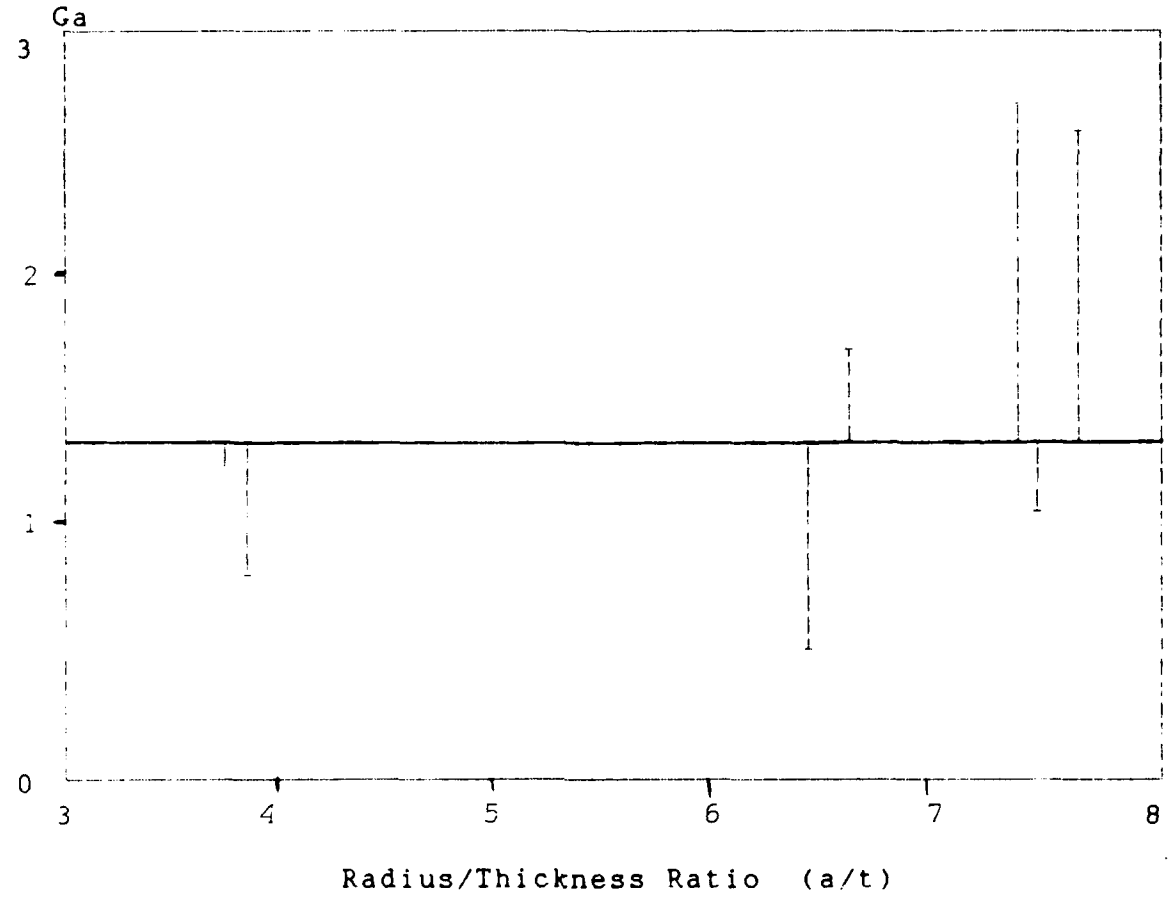

Figure 34. Plot of Adhesive Fracture Energy versus Blister Radius/Thickness Ratio * for all Plexiglass Substrates

* Horizontal line represents the mean value.
Vertical lines represent deviation of experimental data from the mean value.

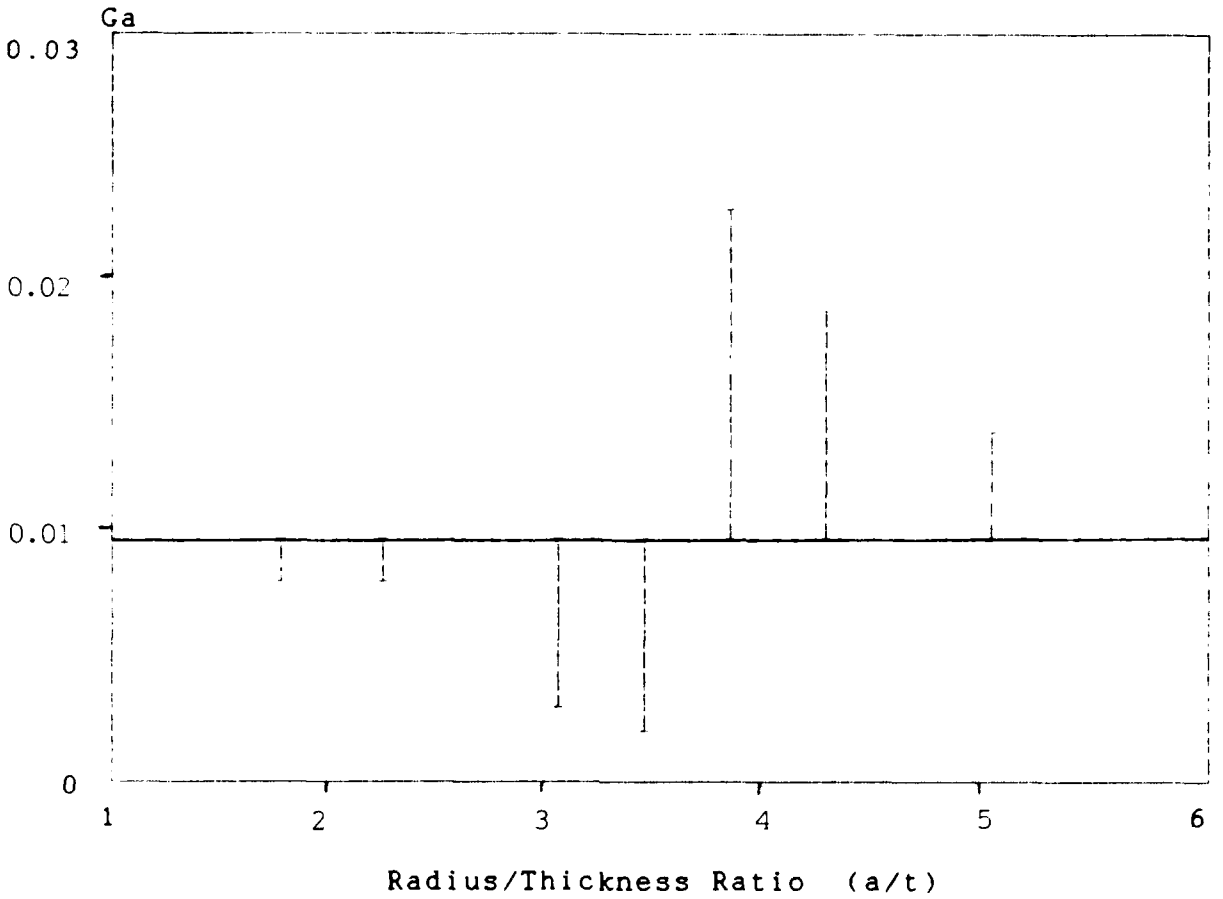

Figure 35. Plot of Adhesive Fracture Energy versus Blister Radius/Thickness Ratio * for all Unpolished Crystal Substrates

* Horizontal line represents the mean value.
Vertical lines represent deviation of experimental data from the mean value.

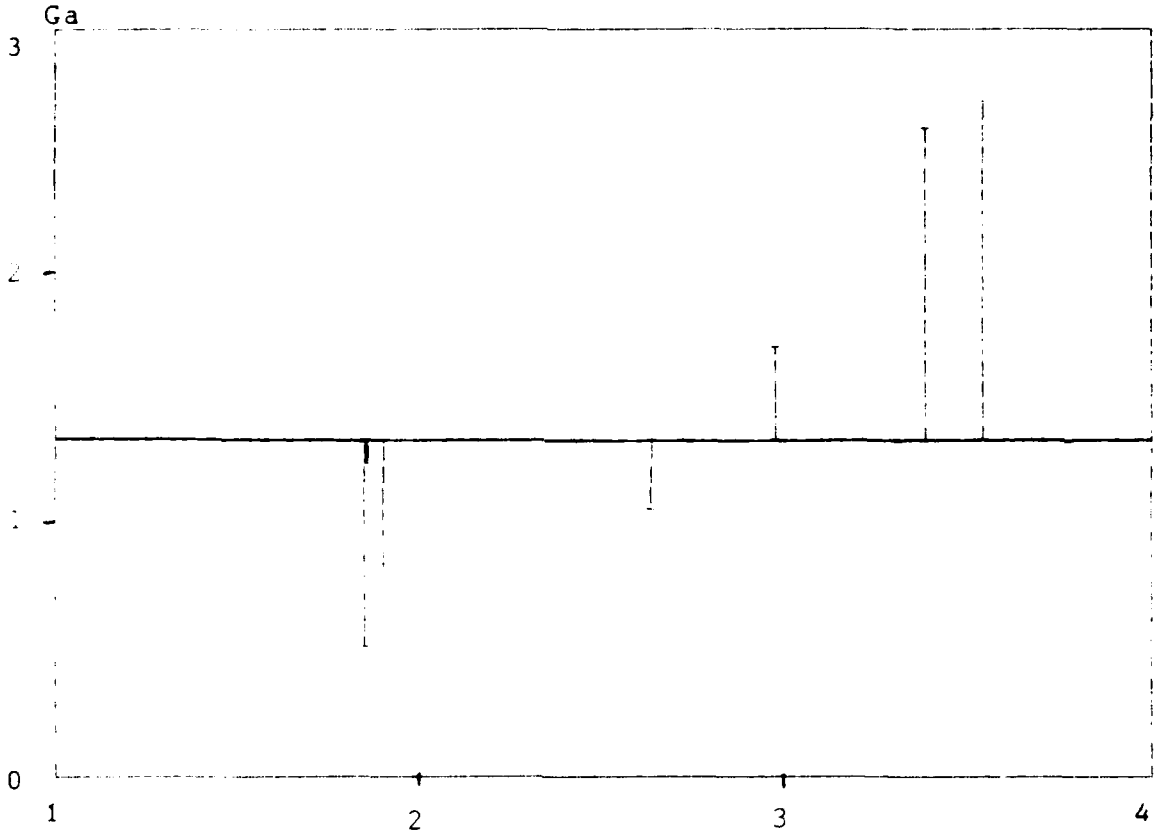

Figure 36. Plot of Adhesive Fracture Energy versus Blister Deflection/Thickness Ratio * for all Plexiglass Substrates

* Horizontal line represents the mean value.
Vertical lines represent deviation of experimental data from the mean value.

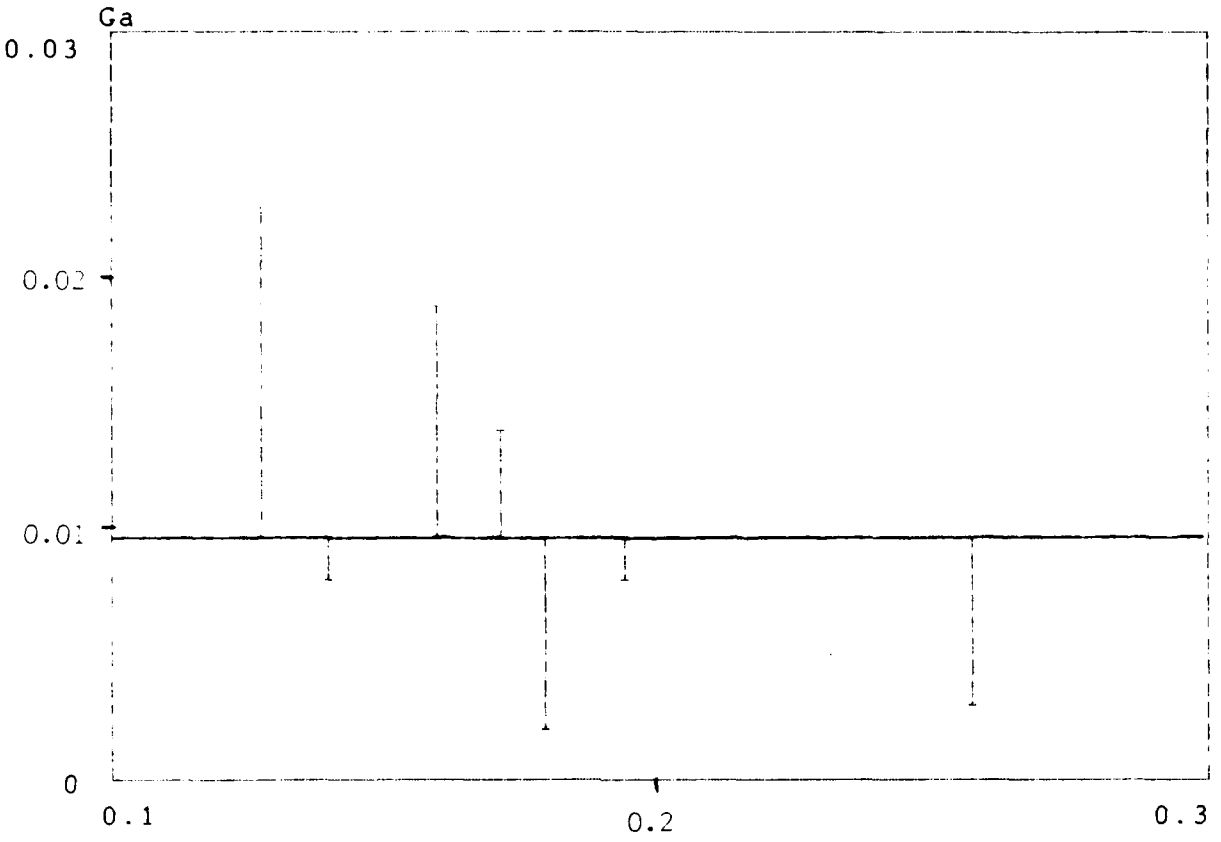

Figure 37. Plot of Adhesive Fracture Energy versus Blister Deflection/Thickness Ratio * for all Unpolished Crystal Substrates

* Horizontal line represents the mean value.
Vertical lines represent deviation of experimental data from the mean value.

Vita

Captain James N. Hanley [redacted] In May 1980, he received a Bachelor of Science degree in Engineering Mechanics from the United States Air Force Academy, Colorado and was commissioned in the United States Air Force. He attended Undergraduate Pilot Training at Williams AFB, Arizona and received his wings in July 1981. He was then assigned as a pilot to the 463rd Tactical Airlift Wing, Dyess AFB, Texas, until May 1987. He is presently enrolled at the Air Force Institute of Technology as a Masters of Science degree candidate in Aeronautical Engineering.

[redacted]

REPORT DOCUMENTATION PAGE

Form Approved
OMB No. 0704-0188

1a REPORT SECURITY CLASSIFICATION Unclassified	1b RESTRICTIVE MARKINGS
2a SECURITY CLASSIFICATION AUTHORITY	3 DISTRIBUTION/AVAILABILITY OF REPORT Approved for Public Release; Distribution Unlimited
2b DECLASSIFICATION/DOWNGRADING SCHEDULE	
4 PERFORMING ORGANIZATION REPORT NUMBER(S) AFIT/GAE/AA/88D-19	5 MONITORING ORGANIZATION REPORT NUMBER(S)
6a NAME OF PERFORMING ORGANIZATION School of Engineering 6b OFFICE SYMBOL (If applicable) AFIT/ENY	7a NAME OF MONITORING ORGANIZATION Air Force Astronautics Laboratory
6c ADDRESS (City, State, and ZIP Code) Air Force Institute of Technology Wright-Patterson AFB, Ohio 45433	7b ADDRESS (City, State, and ZIP Code) Edwards AFB California 93523-5000
8a NAME OF FUNDING/SPONSORING ORGANIZATION AFAL/MKPB 8b OFFICE SYMBOL (If applicable) AFAL/MKPB	9 PROCUREMENT INSTRUMENT IDENTIFICATION NUMBER Advice No: 588-988
8c ADDRESS (City, State, and ZIP Code) Edwards AFB, California 93523-5000	10 SOURCE OF FUNDING NUMBERS PROGRAM ELEMENT NO: 6230 2F PROJECT NO: 6698 TASK NO: 5730 WORK UNIT ACCESSION NO: B8

11 TITLE (Include Security Classification)

Internal Debonding of Solid Rocket Fuel: An Experimental Investigation (Unclassified)

12 PERSONAL AUTHOR(S)
Hanley, James Niles, B.S., Captain, USAF

13a TYPE OF REPORT	13b TIME COVERED	14 DATE OF REPORT (Year, Month, Day)	15 PAGE COUNT
MS Thesis	FROM _____ TO _____	1988 December	109

16 SUPPLEMENTARY NOTATION

17 COSATI CODES			18 SUBJECT TERMS (Continue on reverse if necessary and identify by block number)
FIELD	GROUP	SUB-GROUP	
11	01		Adhesive Fracture Energy Blister Test

19 ABSTRACT (Continue on reverse if necessary and identify by block number)

The objective of this study was the development of a method to compute the fracture energy required to debond crystal particles in a solid rocket fuel. A blister test was defined that pressurizes an initially debonded region to generate an adhesive fracture. An LVDT measures the displacement of the blister. The fracture energy is expressed in terms of the critical loading, displacement, specimen geometry and material properties. Consistent results required developing a proper casting and curing method for thin polymeric layers onto a crystal substrate. Various thicknesses and substrates were examined.

The study found that the deflection of the blister behaved like a plate and could be analyzed as one to compute the adhesive fracture energy. The dimensionless values of fracture energy fell along predictable curves for small values of adhesive thicknesses to blister radii. The adhesive fracture energy was found to be a function of force applied, adhesive material properties and blister geometry.

The value for adhesive fracture energy on a crystal substrate is compared (continued on the back)

20 DISTRIBUTION/AVAILABILITY OF ABSTRACT	21 ABSTRACT SECURITY CLASSIFICATION	
☒ UNCLASSIFIED/UNLIMITED ☐ SAME AS RPT ☐ DTIC USERS	Unclassified	
22a NAME OF RESPONSIBLE INDIVIDUAL Paul D. Copp, Maj, USAF	22b TELEPHONE (Include Area Code) 513-255-2362	22c OFFICE SYMBOL AFIT/ENY

Abstract continued:

to a Plexiglass substrate for an epoxy resin. And a polished and unpolished crystal specimen's fracture energy are compared.